Technical University of Denmark

DTU

High temperature proton exchange membranes based on polybenzimidazoles for fuel cells

Li, Qingfeng; Jensen, Jens Oluf; Savinell, Robert F; Bjerrum, Niels J.

Link back to DTU Orbit

DTU Library
Technical Information Center of Denmark

High temperature proton exchange membranes based on polybenzimidazoles for fuel cells

Qingfeng Li [a,*], Jens Oluf Jensen [a], Robert F. Savinell [b], Niels J. Bjerrum [a]

[a] Energy and Materials Science Group, Department of Chemistry, Technical University of Denmark, Kemitorvet 207, DK-2800 Kgs. Lyngby, Denmark
[b] Department of Chemical Engineering, Case Western Reserve University, Cleveland, OH, USA

ARTICLE INFO

ABSTRACT

To achieve high temperature operation of proton exchange membrane fuel cells (PEMFC), preferably under ambient pressure, acid–base polymer membranes represent an effective approach. The phosphoric acid-doped polybenzimidazole membrane seems so far the most successful system in the field. It has in recent years motivated extensive research activities with great progress. This treatise is devoted to updating the development, covering polymer synthesis, membrane casting, physicochemical characterizations and fuel cell technologies. To optimize the membrane properties, high molecular weight polymers with synthetically modified or N-substituted structures have been synthesized. Techniques for membrane casting from organic solutions and directly from acid solutions have been developed. Ionic and covalent cross-linking as well as inorganic–organic composites has been explored. Membrane characterizations have been made including spectroscopy, water uptake and acid doping, thermal and oxidative stability, conductivity, electro-osmotic water drag, methanol crossover, solubility and permeability of gases, and oxygen reduction kinetics. Related fuel cell technologies such as electrode and MEA fabrication have been developed and high temperature PEMFC has been successfully demonstrated at temperatures of up to 200 °C under ambient pressure. No gas humidification is mandatory, which enables the elimination of the complicated humidification system, compared with Nafion cells. Other operating features of the PBI cell include easy control of air flow rate, cell temperature and cooling. The PBI cell operating at above 150 °C can tolerate up to 1% CO and 10 ppm SO_2 in the fuel stream, allowing for simplification of the fuel processing system and possible integration of the fuel cell stack with fuel processing units. Long-term durability with a degradation rate of 5 μV h^{-1} has been achieved under continuous operation with hydrogen and air at 150–160 °C. With load or thermal cycling, a performance loss of 300 μV per cycle or 40 μV h^{-1} per operating hour was observed. Further improvement should be done by, e.g. optimizing the thermal and chemical stability of the polymer, acid–base interaction and acid management, activity and stability of catalyst and more importantly the catalyst support, as well as the integral interface between electrode and membrane.

© 2009 Elsevier Ltd. All rights reserved.

Contents

* Corresponding author. Tel.: +45 45252318; fax: +45 45883136.
  E-mail address: lqf@kemi.dtu.dk (Q. Li).

1. Introduction

1.1. High temperature PEMFC

Fuel cells are electrochemical devices with high energy conversion efficiency, minimized pollutant emission and other advanced features. Proton exchange membrane fuel cell (PEMFC), among the five types of fuel cells, is attractive both for automobile and stationary applications.

Compared to liquid electrolyte systems, the essentially solid proton exchange membranes have numerous advantages. They are simple to handle, compact, amenable to mass production, can be fabricated into very thin films with excellent resistance to permeation of gaseous reactants. In addition, a solid polymer membrane being strong and yet elastic is a major structural component in the cell. It makes the handling, sealing and assembling much easier than for fuel cells with liquid electrolytes. Moreover, it improves the pressure imbalance tolerance between half-cells.

For most PEMFCs the proton exchange membranes are currently based on perfluorosulphonic acid (PFSA) polymers, e.g. Nafion® [1]. This membrane material has high conductivity, excellent chemical stability, mechanical strength and flexibility, and potentially long-term durabil-

ity. However, it functions only in a highly hydrated state and therefore it is limited to operation at temperatures up to around 80 °C under ambient pressure in order to maintain a high water content in the membrane.

Several challenges for the PEMFC power technology are associated with low operating temperature [2]. Fuel processors, i.e. hydrogen storage tanks and hydrocarbon or alcohol reformers with subsequent CO removers are voluminous, heavy, costly and in most cases complex. Water management involves appropriate humidification of fuel and oxidant, airflow rate and power load regulation. Temperature control or cooling is more critical for larger stacks, and the heat is of low value.

PEMFC operating at high temperatures has in recent years been recognized as a promising solution to meet these technical challenges [2]. The term *high temperature* used here refers to a temperature range from 100 to 200 °C, relative to the well-developed PEMFC technology typically operating at 80 °C (it should be noted that fuel cells working at temperatures up to 200 °C still belong to the overall class "low temperature fuel cells" in contrast to molten carbonate fuel cells and solid oxide fuel cells). Though this temperature range does not seem high in any engineering sense, it is indeed a big stride for the development of proton exchange polymer membranes, both from materials sci-

Nomenclature

AB-PBI	poly(2,5-benzimidazole)
APU	auxiliary power unit
COS	compound of organo-sulphur
CHP	combined heat and power
DABA	3,4-diaminobenzoic acid
DBpX	dibromo-p-xylene
DSC	differential scanning calorimetry
DIB	1,4-diiodobutane
DMAc	dimethylacetamide
DMSO	dimethyl sulphoxide
DMF	N,N-dimethylforamide
DMFC	direct methanol fuel cell
DOA	dodecylamine
DPIP	diphenyl isophthalate
DTA	differential thermal analysis
EGDE	ethylene glycol diglycidyl ether
F_6-PBI	hexafluoro PBI
FT-IR	Fourier transform infrared spectrometry
GDL	gas diffusion layer
GDE	gas diffusion electrode
HOR	hydrogen oxidation reaction
HPA	heteropolyacids
IEC	ion exchange capacity
IPA or mIPA	meta-isophthalic acid
IR	infrared
IV	inherent viscosity
MAS	magic-angle spinning
MEA	membrane–electrode assembly
MMT	modified montmorillonite
MS	mass spectrometry
MSA	methanesulphonic acid
M_W	weight averaged molecular weight
NMP	N-methylpyrrilidone
NMR	nuclear magnetic resonance
OCV	open circuit voltage
OO-PBI	PBI containing 2 ethers
ORR	oxygen reduction reaction
OSO_2-PBI	ether and sulphone containing PBI
PA	phosphoric acid
PAFC	phosphoric acid fuel cell
PAAM	polyacrylamide
PBI or mPBI	poly[2,2′-(m-phenylene)-5,5′-bibenzimidazole]
PEEK	polyetheretherketone
PEI	polyethyleneimine
PEM	proton exchange membrane (polymer electrolyte membrane)
PEMFC	proton exchange membrane fuel cell (polymer electrolyte membrane fuel cell)
PEO	polyethylene oxides
PFSA	perfluorosulphonic acid
POD	polyoxadiazole
PPA	polyphosphoric acid
pPBI	poly[2,2′-(p-phenylene)-5,5′-bibenzimidazole]
PPO	polyphenylene oxide, especially poly(2,6-dimethyl-1,4-phenylene oxide

PSF	polysulphone
PTA or PWA	phosphotungstic acid
PTFE	polytetrafluoroethylene
PVDF	polyvinylidene difluoride
PVP	poly(vinylpyrrolidone)
P_4VP	poly(4-vinylpyridine)
PVPA	polyvinylphosphonic acid
PWA or PTA	phosphotungstic acid
Py-PBI	pyridine containing PBI
Py-O-PBI	pyridine-based PBI containing ether
RH	relative humidity
SiWA (STA)	silicotungstic acid
SO_2-PBI	sulphone containing PBI
SPBI	sulphonated poly [2,2′-(m-phenylene)-5,5′-bibenzimidazole]
SPEEK	sulphonated polyetheretherketone
SPOP	sulphonated poly[bis(phenoxy)phosphazene]
SPPO	sulphonated polyphenylene oxide, especially poly(2,6-dimethyl-1,4-phenylene oxide)
SPSF	sulphonated polysulphone
TAB	tetraaminobiphenyl (or DAB—diaminobenzidine)
TCDA	tetracarboxylic dianhydride
TADE	3,3′,4,4′-tetraaminodiphenyl-ether
T_g	glass transition temperature
TFA	trifluoroacetic acid
TGA	thermogravimetric analysis
THF	tetrahydrofuran
TPA or pTPA	para-terephthalic acid
TPAH	terephthaldehyde
VPA	vinylphosphonic acid
ZrP	zirconium hydrogen phosphate
Zr(PBTC)	zirconium tricarboxybutylphosphonate $(Zr(O_3PC(CH_2)_3(COOH)_3)_2$

ence and technological points of view. First of all, elevated temperatures tend to stress the critical issues of thermal, chemical and mechanical stabilities of polymer materials. Secondly the proton conductivity usually involves a "vehicle" or a "hopping" mechanism with help of water molecules, which are also an inevitable product of any fuel cell system. Above 100 °C water evaporates under ambient pressure. An increase in operating temperature from 80 to 200 °C will lead to a saturated water vapour pressure of as high as 15 atm, resulting in great complexity of the system construction if high relative humidity is to be achieved during operation. Thirdly, the cooling design and efficiency of a fuel cell stack depends on the temperature difference between the stack and the atmosphere. A temperature increase from 80 to 200 °C may mean 3–4 times reduction in the front area of radiators, which is another key issue of the power system especially for automobile applications. Finally and probably most importantly, this temperature increase can dramatically enhance the electrode tolerance to fuel impurities (e.g. CO and sulphide). The enhanced tolerance to the fuel impurities and the availability of high temperature heat will decisively simplify
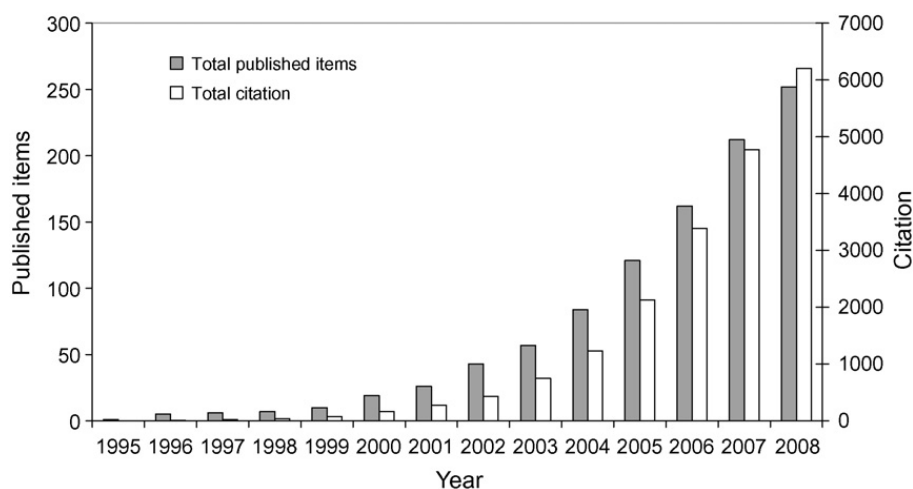
Fig. 1. Accumulative published items and citations of the topic "polybenzimidazole" and "fuel cells" indexed within Web of Science (November 4, 2008).

the fuel processing units and improve the overall system efficiency.

Great efforts have been and are being made to develop proton conducting membranes and other materials for operation at temperatures above 100 °C [2–5]. Membranes under active development can be classified into the following groups and have been well reviewed in recent years: (1) modified perfluorosulphonic acid (PFSA) membranes [2,3]; (2) alternative membranes based on partially fluorinated and aromatic hydrocarbon polymers [6–9]; (3) inorganic–organic composites [10–12]; (4) acid–base polymer membranes [13–16], typically a basic polymer doped with a non-volatile inorganic acid or blended with a polymeric acid. As the focus of this treatise, discussion below is restricted to the acid–base membranes.

### 1.2. Acid-doped polybenzimidazole membranes

Acid–base complexation represents an effective approach to development of proton conducting membranes. Polymers bearing basic sites like ether, alcohol, imine, amide, or imide groups react with strong or medium strong acids. The basic polymer acts as a proton acceptor like in a normal acid–base reaction, and an ion pair is formed. The polymers used in earlier investigations include polyethyleneoxide (PEO), polyacrylamide (PAAM), poly(vinylpyrrolidone) (PVP), polyethyleneimine (PEI), and others, as summarized by Lasségues [17]. It seems that high conductivity can only be obtained with amphoteric acids, especially phosphoric or phosphonic acids.

From proton conducting mechanism points of view, phosphoric and phosphonic acids are interesting because they are more amphoteric, having both proton donor (acidic) and proton acceptor (basic) groups to form dynamic hydrogen bond networks, in which protons can readily transfer by hydrogen bond breaking and forming processes, as recently rationalized by Kreuer and co-workers [18–20]. Other important features of phosphoric or phosphonic acids are their excellent thermal stability and low vapour pressure at elevated temperatures.

Most of these acid–polymer combinations from the early work exhibit proton conductivity less than

10^{-3} S cm^{-1} at room temperature. If the acid content is higher, the plastifying effect of the excessive acid leads to the formation of a soft paste, unable to be processed into membranes. A breakthrough was achieved when polybenzimidazole (PBI) was first proposed for preparing acid-doped membranes [21]. Since then phosphoric acid-doped PBI membranes have been successfully developed and systematically characterized. The first patent was filed by Savinell and Litt [22], after which numerous patents on PBI membranes and fuel cells have been issued to Savinell's group [23], Hoechst Celanese and Aventis [24], Honda [25], Motorola [26], Danish Power Systems [27], Plug Power [28], among others. High conductivity [29–33], good mechanical properties [34] and excellent thermal stability [35] have been reported at temperatures up to 200 °C under ambient pressure. Fuel cells and related technologies have been developed with operating features such as little humidification [36], high CO tolerance [37], better heat utilization [38,39] and possible integration with fuel processing units [40,41]. Modelling has been carried out for PBI cells with respect to mass transport and polarization phenomena [42–46] as well as system dynamics and design [47–50].

In recent years extensive research activities have been motivated and great progress has been made, as seen from Fig. 1. From a technological application point of view, PBI-based fuel cells seem most suited for stationary power applications, for example, based on natural gas reforming and combined heat and power (CHP) generation [51]. For automobile applications more challenges exist by considering startup time and thermal/load cycling, however, an auxiliary power unit (APU)-like system is of special interest. Volkswagen has at the 2007 Los Angeles Motor Show presented a hybrid concept car with a PBI stack as a charger for batteries to extend the driving range. As small power units, the PBI-based cells have the potential to integrate with a simplified methanol reformer or metal hydride tank. In addition, this proton conducting polymer electrolyte opens the door for many other electrochemical applications that could benefit from or require higher temperatures such as hydrogen gas pumping and purification [52], electrochemical sensors [53–55] and water electrolysis. The present
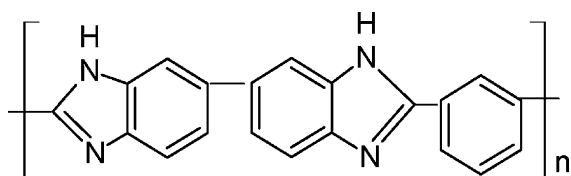
Scheme 1. Poly 2,2′-*m*-(phenylene)-5,5′-bibenzimidazole.

treatise attempts to update the development covering polymer synthesis, acid doping, physicochemical characterizations, and to a brief extent fuel cell technologies.

2. Polymer synthesis and membrane fabrication

The term PBI is today used in two ways. In a wide definition PBI refers to a large family of aromatic heterocylic polymers containing benzimidazole units. PBI with different structures can be synthesized from hundreds of combinations of tetraamines and diacids. In a specific way PBI refers to the commercial product under the trademark Celazole®, poly 2,2′-*m*-(phenylene)-5,5′-bibenzimidazole (Scheme 1). In the context of PBI with different structures this specific PBI is also named as *m*PBI because the phenylene ring is meta-coordinated.

As an amorphous thermoplastic polymer, the aromatic nuclei of PBI provide the polymer high thermal stability (glass transition temperature, T_g = 425–436 °C), excellent chemical resistance, retention of stiffness and toughness, however, with poor processability, as reviewed previously [56–58]. Primarily used in textile fibres, the selection of poly 2,2′-*m*-(phenylene)-5,5′-bibenzimidazole as the commercial product was made on the basis of its good fibre properties, availability of monomers and identification of suitable solvents for fibre extrusion. As a specialty polymer PBI has also been used as compression moulding resin, electrically conductive materials by impregnation of, e.g. metal sulphide [59,60], casting films and coatings for liquid [61–67], gas [68–70] and other [71–75] separation purposes.

For fuel cell uses, more efforts have recently been made to modify the polymer structures. One motivation of these efforts is to improve the properties such as high molecular weight and good solubility and processibility, which are of significance for mechanical stability and functionalization processing of PBI membranes. Another motivation is to tailor the basicity of the polymers for improving the acid–base membranes. These modifications are accomplished in two ways, either by synthetically modifying the monomers

prior to polymerization or by the post-polymerization substitution of the polymer at the reactive benzimidazole N–H sites. In this section, a brief introduction to the polymer synthesis is first made, followed by a discussion on the recent efforts for PBI modifications.

2.1. Monomers and polymer synthesis

2.1.1. Heterogeneous molten/solid state synthesis

In 1961, Vogel and Marvel [76] reported the first synthesis of PBI by heating an equimolar mixture of bis(*o*-diamine)s and the phenyl esters of different dicarboxylic acids. Based on it, a two stage process was developed to produce PBI with tetraaminobiphenyl (TAB) and diphenyl isophthalate (DPIP) as monomers [56], as shown in Scheme 2.

The first step is carried out at about 270 °C to produce the low molecular weight prepolymer in form of voluminous foams. The prepolymer is then pulverized and further heat-treated at temperatures of up to 360 °C to increase the molecular weight of the polymer by further polymerization. In general this is an inconvenient process because the prepolymer has to be discharged and pulverized before the second step. By replacing DPIP with isophthalic acid (IPA) in the presence of organo phosphorus and silicon compounds as catalysts, Choe [77,78] developed a single stage method to synthesize high molecular PBI (see Scheme 3):

The synthesized polymer is often characterized in terms of molecular weight by measurement of the inherent viscosity (IV, in dL g^{-1}) of a polymer solution in concentrated sulphuric acid. The inherent viscosity is related to the weight averaged molecular weight (M_W, in g mol^{-1}) of the polymer by the Mark–Houwink–Sakurada equation:

$$IV = K - M_W^{\alpha} \tag{1}$$

For PBI dissolved in 96 wt% H_2SO_4 at a concentration of 0.5 g of the polymer in 100 mL acid at room temperature, the empirical constants K and α are 1.94×10^{-4} and 0.79, respectively.

As a result of the heterogeneous polycondensation at elevated temperatures, the commercially available polymer has limited molecular weight or IV in order to avoid the polymer being insoluble or infusible. For example, commercial PBI (Celazole®) with a low to medium molecular weight of M_W from 23,000 to 37,000 g mol^{-1}, corresponding to an IV of ca. 0.55–0.8 dL g^{-1}, was introduced mainly for moulding resin applications [79].
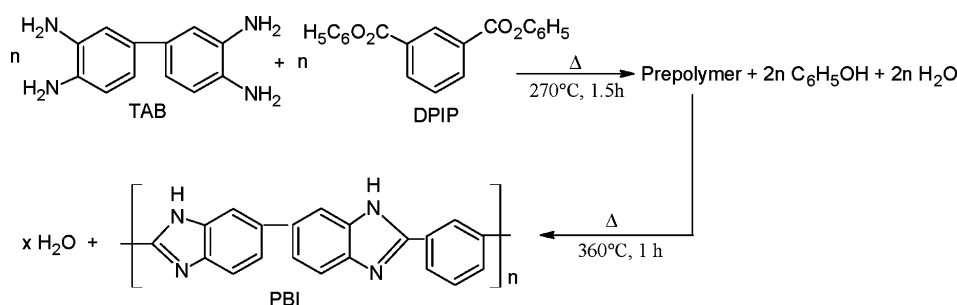
Scheme 2. The two-stage process for PBI synthesis.
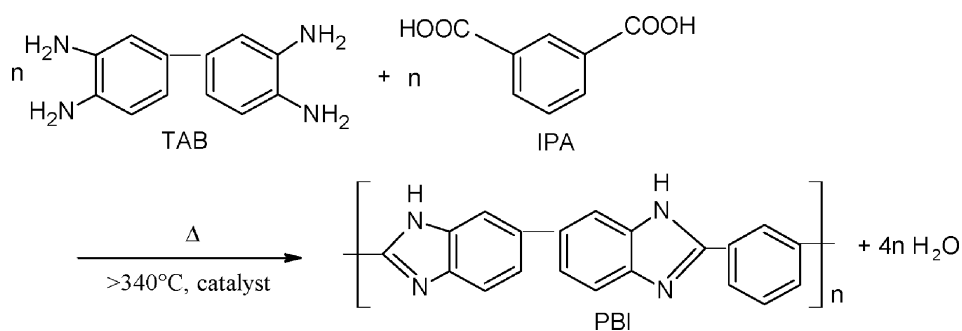
Scheme 3. The single-stage process for PBI synthesis.

For membrane casting purposes, high molecular weight polymers are desirable in order to achieve mechanically stable membranes at higher acid-doping levels and therefore high proton conductivities. As to be discussed in Section 2.2, PBI membranes can be directly cast from acid solutions. High molecular weight of polymers is essential for those directly cast membranes. Based on the commercial polymer products, fractionation and extraction of high IV PBI seem necessary. By dissolving the low molecular weight component in DMAc at temperatures from 94 to 160 °C, Wainright et al. [13] obtained the undissolved high molecular polymer.

2.1.2. Homogeneous solution synthesis

PBI can also be synthesized in homogeneous solutions with solvents such as polyphosphoric acid (PPA) [80] (see Scheme 4). Taking advantages of a moderate temperature (170–200 °C) and using more stable monomers (TAB stabilized by tetra hydrochloride), this method is an excellent route for preparing laboratory or small scale batches of linear, high molecular weight polymers, though a relatively large amount of acid solvent and multiple-step isolation procedures are involved. In the discussion of the following section (Section 2.1.3) almost all syntheses of modified PBIs were made in PPA.

Attempts have been made to introduce phosphorus-based catalysts, e.g. triphenyl phosphate in the PPA synthesis [81], however, it seems that temperature, monomer purity and removal of oxygen traces in the reactor are more important for obtaining high molecular weight polymers.

Other solvents than PPA have also been used for the homogeneous synthesis of PBI. Molten sulpholane or diphenyl sulphone was suggested in the early years [82]. Eaton et al. [83] proposed a mixture of phosphorus pentoxide (P_2O_5) and methanesulphonic acid (MSA) as the solvent,

which is a low-viscous liquid, suitable for the homogeneous synthesis and the following acid-washing. This P_2O_5–MSA mixture has recently been employed by Kim et al. [84] and Jouanneau et al. [85].

2.1.3. PBI with synthetically modified structures

The extensive work on synthetically modified PBI from early years was well reviewed [56,57] with comprehensive listing of monomers of varied structures, which primarily consist of bis(3,4-tetraaminodiphenyl) containing ether, sulphone, ketone and aliphatic groups and various bis(phenoxycarbonyl) acid derivatives. Below is a brief discussion on those polymers prepared in recent years for fuel cell applications.

2.1.3.1. para PBI.
Poly[2,2′-*p*-(phenylene)-5,5′-bibenzimidazole] (*p*PBI, Scheme 5a) was first synthesized in the early 1960s [76,80] and seems of more interest in recent years [86–89]. Compared with the *meta*-PBI, the *para* structure of the polymer showed superior tensile strength and stiffness [90], however, the glass transition temperature was lowered by 59 °C [57], indicating the enhanced flexibility of the polymer chain due to introduction of the p-phenylene linkage in the backbone. The synthesis is done by using *para*-terephthalic acid (TPA) instead of *meta*-isophthalic acid (IPA). Using TPA was found to be able to increase the molecular weight of the polymer, though its solubility in PPA is low (<4%). Xiao et al. [89] reported that under identical conditions, the synthesized *m*PBI has the IV values ranging from 1.3 to 2.0 dL g^{-1} while the *p*PBI has an IV value from 1.5 to 3.0 dL g^{-1}.

2.1.3.2. Pyridine-based PBI.
Polar pyridine groups as a main chain linkage of aromatic copolymers have been proposed by Kallitsis and Gourdoupi [91,92] for preparing
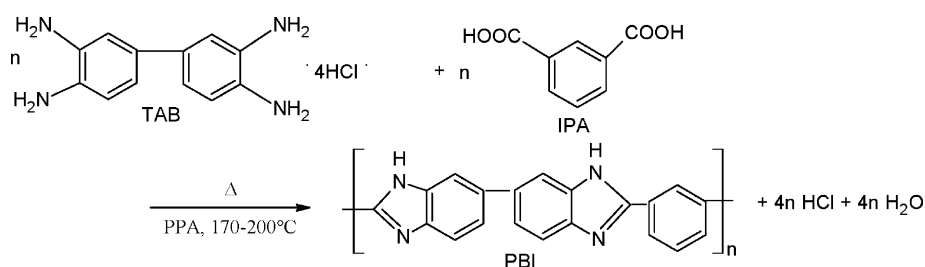
Scheme 4. The PPA process for PBI synthesis.
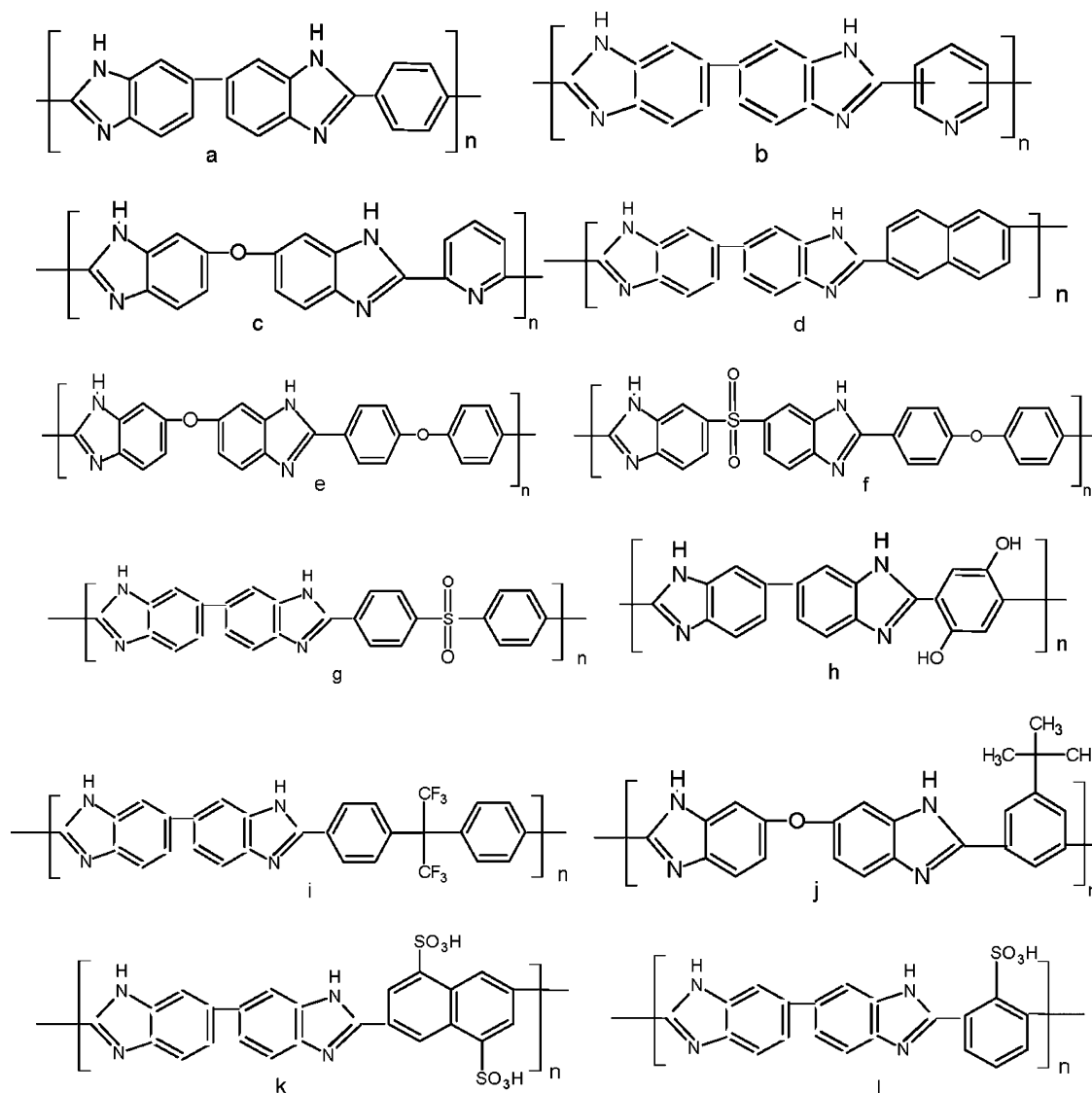
Scheme 5. Various structures of synthetically modified PBI: (a) *para* PBI; (b) Py-PBI; (c) Py-O-PBI; (d) naphthalin-PBI; (e) OO-PBI; (f) OSO_2-PBI; (g) SO_2-PBI; (h) 2OH-PBI; (i) F_6-PBI; (j) tert-butyl PBI; (k) sulphonated naphthalin-PBI; (l) sulphonated PBI.

blend membranes. The blend membranes have improved chemical stability against oxidative degradation. Xiao et al. [88,89] found that, when the phenyl ring was substituted by the pyridine ring, the incorporation of an extra nitrogen atom in the polymer significantly improves the solubility. In addition, PBI structures with different numbers of N atoms or NH groups are of special interest for enhancing the acid doping and proton conductivity. Pyridine groups have been incorporated into the PBI main chain as an additional nitrogen containing aromatic heterocycle, in order to increase the base content of the polymer while retaining the inherently high thermo-oxidative stability of the polymer. Pyridine-based PBI (Py-PBI, Scheme 5b) has been synthesized from the pyridine dicarboxylic acids by several groups [89,93,94]. Xiao et al. [89] used 2,4-, 2,5-, 2,6-, and 3,5-pyridine dicarboxylic acids to synthesize the corresponding pyridine-based PBIs. Schuster et al. [94] synthesized PBI containing both pyridine and ether (Py-O-PBI, Scheme 5c) from equimolar amounts of 2,6-pyridine-dicarboxylic acid and 3,3′,4,4′-tetraaminodiphenyl-ether (TADE) in PPA.

2.1.3.3. AB-PBI.
Poly(2,5-polybenzimidazole) (AB-PBI) has a simpler structure than PBI without the connecting phenyl rings and therefore a high concentration of the basic sites in the structure. It can be polymerized from a single monomer (3,4-diaminobenzoic acid) (DABA, Scheme 6), which is less expensive, commercially available (e.g. used in the pharmaceutical industry) and non-carcinogenic. Recent efforts to synthesize AB-PBI are made in polyphosphoric acid [13,15,94,95] or in a P_2O_5–MSA mixture [84]. As the unbalancing of stoichiometry is avoided, the synthesis would be less demanding for the purity of the monomer. It is, however, reported that the high purity monomer gives polymers of high molecular weights [13,95]. By using
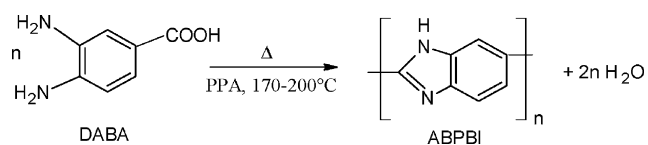
Scheme 6. The synthesis of AB-PBI.

recrystallized DABA, Wainright et al. [13] synthesized AB-PBI with an inherent viscosity as high as 7.33, which is essential to prepare PBI membranes by direct casting (see Section 2.2.1) from a PBI solution in trifluoroacetic acid (TFA)-PA mixture. Asensio and Gomez-Romero [15] suggested that an inherent viscosity of an AB-PBI solution in concentrated sulphuric acid should be higher than $2.3\,dL\,g^{-1}$ in order to cast good enough membranes by direct casting from an MSA solution [15] or an MSA-PA mixture [96]. In addition, AB-PBI has a higher affinity towards acids than PBI, allowing for doping with phosphoric acid and sulphonation by sulphuric acid.

2.1.3.4. Other modifications of main chains. Carollo et al. [93] synthesized a series of PBIs with different numbers of N-atoms, i.e. different basicities, including, among others, poly(2,2′-(2,6-naphthalin)-5,5′-bibenzimidazole) (naphthalin-PBI, Scheme 5d) and poly(2,2′-(2,6-pyridin)-5,5′-bibenzimidazole) (Py-PBI, Schemes 5b). They found that both the acid-doping level and the proton conductivity remarkably increased with the membrane molecular weight and basicity, which depend on the amount of NH-groups as well as on their position in the polymer backbone.

Schuster et al. [94] has, in addition to Py-O-PBI (Scheme 5c), synthesized OO-PBI (Scheme 5e) and OSO_2-PBI (Scheme 5f). The OO-PBI was synthesized by a standard polycondensation reaction of 3,3′,4,4′-tetraaminodiphenyl-ether (TADE) and 4,4′-oxy-dibenzoic acid. And the OSO_2-PBI was synthesized from 3,3′,4,4′-tetraaminodiphenyl-sulphone and 4,4′-oxy-dibenzoic acid. Similarly Qing et al. [97] prepared sulphone containing PBI (Scheme 5g) by using 4,4′-sulphonyldibenzoic acid. In general the polymers containing ether, sulphone, etc., would have lowered thermo-oxidative stability but increased solubility and flexibility, which allow further processing, modification (cross-linking, sulphonation to high ion exchange capacity (IEC)) and production of films with good mechanical properties.

By using a variety of diacids, more synthesis has been made of PBI with modified structures. Dihydroxy-PBI (Scheme 5h) was synthesized [98] and found to be insoluble in concentrated sulphuric acid. Membranes by direct casting of the polymer solution in polyphosphoric acid showed much higher conductivity

than the corresponding *para*-PBI membranes. Using 4,4-(hexafluoroisopropylidene)bis(benzoic acid) [70,99,100], hexafluoro PBI (F_6-PBI, Scheme 5i) has been prepared, showing good organosolubility. Similarly PBI containing *tert*-butyl groups (*tert*-butyl PBI, Scheme 5j) has also been prepared from 5-*tert*-butyl isophthalic acid [70]. These diacids can also be sulphonated first, for example, in form of 4,8-disulphonyl-2,6-naphthalenedicarboxylic acid [101] or 5-sulphoisophthalic acid [97], as a way to prepare sulphonated PBI membranes (Scheme 5k and l). Copolycondensation of a sulphonated aromatic diacid and a non-sulphonated aromatic diacid with an aromatic tetraamine [97,101–103] has also been investigated as a way to avoid the side reactions and to control the sulphonation degree. Recently and interestingly, Xu et al. [104,105] synthesized a series of amine-terminated hyperbranched PBI. With help of cross-linkers during solution casting, strong membranes were obtained.

2.1.4. PBI modified by post-polymerization substitution
2.1.4.1. N-substituted PBI. The NH groups in the imidazole rings are chemically reactive. For some applications the chemical reactivity can be reduced by, e.g. replacement of the hydrogen of the imidazole ring with less reactive substituents such as hydroxyethyl [106], sulphoalkyl [107,108], cyanoethyl [109], phenyl [110] and alkyl, alkenyl or aryl [111] groups. The methods developed by Sansone et al. [107–111] use a PBI solution in DMAc or *N*-methylpyrrilidone (NMP). The unsubstituted PBI is first reacted with an alkali hydride to produce a polybenzimidazole poly-anion, which is then reacted with a substituted or unsubstituted alkyl, aryl or alkenyl methyl halide to produce an N-substituted PBI, as shown in Scheme 7.

From studies of early years, Cassidy [57] concluded that the substitution of a methyl group onto the amino nitrogen lowers the softening temperature by $140\,°C$, increases solubility by a factor of 5, and decreases thermal stability by $10\,°C$. As a comparison, methyl groups on the aromatic ring of the tetraamine lower the softening temperature by only $10–40\,°C$, indicating the importance of hydrogen bonding that is lost in the N-substituted PBI.

Using the Sansone's method, Klaehn et al. [112] recently prepared a series of N-substituted organosilane ($-CH_2SiMe_2R′$ where R′ = methyl, vinyl, allyl, hexyl, phenyl, and decyl) PBI derivatives with nearly fully sub-
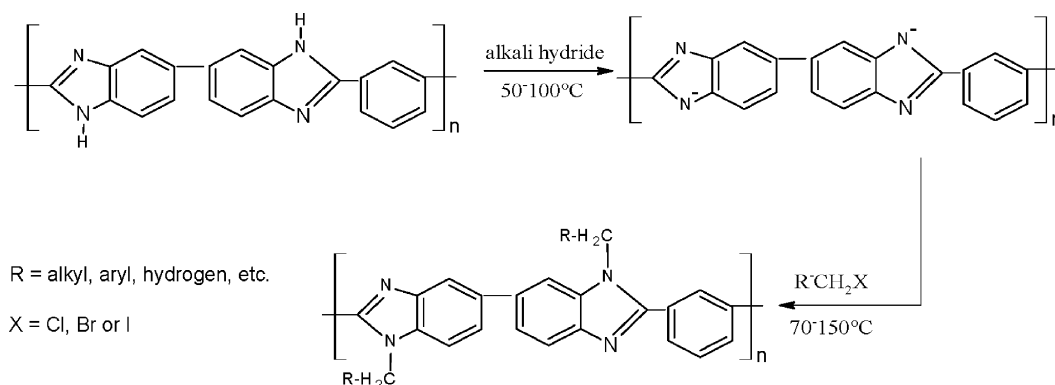
Scheme 7. Post-polymerization N-substitution of PBI.

stitution and very much improved solubility in common organic solvents. Pu and Liu [113–115] prepared poly(*N*-methylbenzimidazole) and poly(*N*-ethylbenzimidazole). Interestingly, when methyl and ethyl groups are introduced on the imidazole moiety, the obtained N-substituted PBI showed high acid-doping levels and therefore high proton conductivity. The authors explained it as a result of the increased basicity of the polymer. However, a more basic polymer should react with the same amount of acid. The actual reason for a higher acid-doping level might be due to the increased polymer spacing or decreased polymer packing when a methyl or ethyl group is introduced, as showed by Kumbharkar et al. [70].
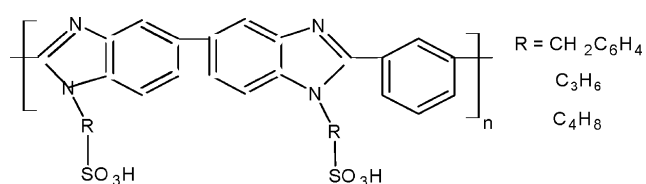
2.1.4.2. Sulphonated PBI. In form of fibres PBI has excellent thermal stability and non-flammability. However, when exposed to a flame, PBI fabric shrinks. In order to minimize the shrinkage at elevated temperatures, the polymer might be post-treated with aqueous sulphuric acid, followed by thermal treatment, to form a salt with the imidazole ring. The obtained so-called *stabilized* PBI, with a sulphonation degree as high as 75%, shows improved dimensional stability. However, this *post-sulphonation thermal treatment* does not seem to significantly increase the proton conductivity of membranes [116,117], probably due to the strong interaction between protons and nitrogen atoms of the imidazolium ring, which reduces the proton mobility.

An attempt to develop PBI-based polyelectrolyte by grafting functional groups is probably first made by Gieselman and Reynolds [118,119], who improved Sansone's process [107] for producing N-substituted PBI with organo-sulphates. More efforts have been made in recent years using this process [6,7,120–123,125]. PBI is first activated by deprotonating the nitrogen in the benzimidazole rings of the polymer backbone with an alkali metal hydrides, followed by reaction with, for example, sodium (4-bromomethyl)benzenesulphonate [6,121–122], arylsulphonates or alkylsulphonates [123–125] to synthesize N-sulphonated PBI (Scheme 8). The introduction of benzylsulphonic, arylsulphonic or alkylsulphonic acids was found to create proton conductivity with better thermal, chemical and mechanical stabilities compared to those of sulphonic acid groups. The conductivity of benzylsulphonate grafted PBI was reported to be higher than 10^{-2} S cm^{-1} at 25 °C [121], while that of PBI-butanesulphonate was higher than 10^{-2} S cm^{-1} at 160 °C [123] with a humidification temperature at 100 °C, which means a relative humidity of ca. 16%.

In addition, it is interesting that modified PBI containing electron donating linkages such as either in PBI-O and PBI-OO is activated for electrophilic substitution reactions [126]. This allows for a direct post-sulphonation of the poly-

mer in concentrated or fuming sulphuric acid [126,127]. In this way the sulphonic groups can be introduced both into the hydroquinone segment of the polymer chain and the benzimidazole segment. Thus obtained sulphonated PBI-OO membranes display an ionic conductivity of up to 0.08 S cm^{-1} at 120 °C and 100% RH [126].

2.2. Membrane fabrication

PBI has been used in form of membranes for different separation purposes especially at high temperatures and in harsh environments. Early efforts were made to develop PBI semi-permeable membranes for electrodialysis, reverse osmosis or ultrafiltration [61]. For those purposes, PBI membranes are a good candidate due to their excellent chemical stability, mechanical strength, thermal stability, durability and low cost. Recently PBI membranes have also been explored for gas separations [68–70]. As a result of close chain packing due to the structure rigidity and strong hydrogen bonding, PBI membranes are dense, with very low gas permeability. For improving its separation performance, PBI is used as semi-permeable membranes, prepared by coagulation in water and annealed in a non-solvent medium, typically ethylene glycol.

In fuel cells, a membrane serves as an ionic conducting electrolyte, an interfacial environment for electrode reactions, an effective reactant separator as well as a support for catalysts/electrodes. It is therefore essential that such a membrane exhibits, among other properties, optimized gas permeability. For this purpose, dense PBI membranes are prepared by solution casting. PBI dissolves in strong acids, bases and a few organic solvents and membranes can be cast from their solutions accordingly. As the membranes are used in an acid functionalized form to achieve proton conductivities, those membranes cast from an acidic solution already contain the acid and are referred to as *directly cast* membranes. There are 2 types of directly cast membranes, prepared from polyphosphoric acid (PPA, called *PPA-cast membranes*) or a mixture of phosphoric acid and trifluoroacetic acid (TFA, called *TFA-cast membranes*). The membranes cast from an organic solution need to be further doped with phosphoric acid. The typically used organic solvent is *N,N*-dimethylacetamide (DMAc), thus obtained membranes are referred to as *DMAc-cast membranes* in the following discussion.

2.2.1. TFA-cast membranes
PBI is soluble in a mixture of trifluoroacetic acid (TFA) and phosphoric acid [23,34]. PBI powder is first mixed with trifluoroacetic acid. After refluxing for a few hours, a certain amount of H_3PO_4, corresponding to the desired acid-doping level, is then added for dissolution of the PBI. In case that a small amount of H_3PO_4 is needed, water can be added to solubilize the PBI. The obtained solution is then filtered and cast into membranes on a glass plate under nitrogen atmosphere. The membrane is then dried at room temperature under vacuum. Thus obtained *TFA membranes* are in general more rubbery and softer than the *DMAc-cast membranes* [13]. The conductivities are higher. However, high molecular weight (M_W) polymers are needed in order to obtain good mechanical strengths. As high M_W polymer

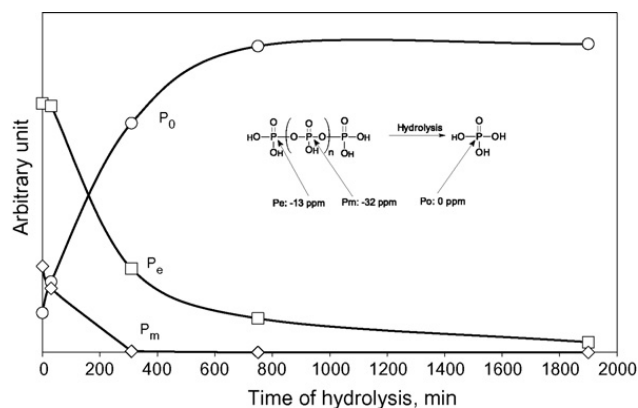**Scheme 8.** Structures of N-sulphonated polybenzimidazoles.

Fig. 2. Change of 31P NMR spectra of directly cast PBI membranes during the PPA hydrolysis (data from [88]).

is essential, more efforts are made to use AB-PBI, which is synthesized from one monomer only with no risk of stoichiometry mismatch.

2.2.2. PPA-cast membranes

As mentioned above, polyphosphoric acid (PPA) is used as an efficient condensation reagent and solvent for the PBI synthesis. Xiao et al. [88,89] developed a sol–gel process to fabricate PBI–H_3PO_4 membranes directly from the PBI solution in PPA at around 200 °C, without isolation or re-dissolution of the polymer after synthesis. After casting, the hydrolysis of PPA to phosphoric acid by moisture from the surrounding environment induces a sol–gel transition (see Fig. 2), resulting in phosphoric acid-doped PBI membranes. In this way acid-doping levels as high as 20–40 mol PA per repeat unit of PBI can be achieved with consequently high conductivity (over 0.2 S cm^{-1}) yet acceptable tensile strength (of up to 3.5 MPa) [88].

It is interesting that the sol–gel behaviours of the PPA membranes depend very much on the polymer structures and molecular weight. High molecular weight or IV of especially *para*-PBI seems to stabilize the gel state and produced membranes with better mechanical stability. Using the pyridine-based PBI, Xiao et al. [88,89] found that 2,5-Py-PBI gives mechanically strong membranes even at an acid level of 25 mol PA per repeat unit of PBI. Among the 3 types of *meta*-Py-PBI investigated, the 3,5 Py-PBI retained all the PA during the hydrolysis process but no sol–gel transition and consequent film formation were observed.

Similarly Kim et al. [128] cast the AB-PBI membranes directly from the synthesis solvent composed of P_2O_5 and MSA. Another attempt by Kim et al. [87] is to directly cast PBI membranes from an MSA solution. They have also tried to quench the directly cast *p*PBI membranes immediately to −20 °C in order to prohibit the formation of *p*PBI crystals. The membrane was, however, washed with water to remove the acid, and the remaining membrane "structure" was then doped with aqueous phosphoric acid.

2.2.3. DMAc-cast membranes and acid doping

PBI is soluble in highly polar, aprotic organic solvents such as DMAc, dimethyl sulphoxide (DMSO), *N,N*-dimethylforamide (DMF), and *N*-methylpyrrilidone (NMP). The typical organic solvent is DMAc.

2.2.3.1. Casting of membranes from DMAc.
A suitable means for dissolving the polymer is to submerge them into a solvent at a temperature above the boiling point of the solvent, for example, 25–120 °C above the boiling point, and at a pressure of 2–15 atm under an oxygen-free atmosphere. The resulting solutions are preferably filtered to remove any undissolved polymer. A minor amount of lithium chloride (typically 2%) may optionally be added to the solution in order to prevent the polymer from separating from the solution during storage for an extended period of time.

PBI membranes can be cast from solutions of different concentrations. After casting onto a glass plate, the majority of the solvent is evaporated in a ventilated oven at temperatures ranging from 60 to 120 °C. The membranes are then washed with hot water in order to remove the stabilizer (LiCl) if any. Strong interaction between the polar groups in PBI and the DMAc molecules makes it difficult to remove the traces of the solvent during the membrane casting. A final drying of the *DMAc-cast membranes* at temperatures of up to 190 °C or under vacuum at lower temperature seems necessary. Similar procedures can be used for casting PBI membranes from other organic solvents. An alternative way is to cast PBI membrane from a mixture of NaOH and ethanol [34].

2.2.3.2. Acid doping.
The DMAc-cast membrane should be doped with acids to become proton conductive. Chemically, PBI is a basic polymer (pK_a = 5.23 as protonated) and can readily react with a strong acid. Various inorganic acids have been investigated such as H_2SO_4 [29–31,129,130], H_3PO_4 [29–34,129–131], $HClO_4$ [129], HNO_3 [129], HBr [29,31], HCl [129]. Among these is phosphoric acid of special interest because of its unique proton conductivity, also under anhydrous conditions, as well as its excellent thermal stability and very low vapour pressure at elevated temperatures.

By immersing a PBI membrane in an aqueous phosphoric acid solution, the equilibrium can be reached after about 50 h at room temperature. Typically an acid-doping level around 5–6 can be achieved by using 65–75 wt% acid solutions. For cross-linked PBI membranes, either covalently or ionically, the acid doping needs to be done at higher acid concentrations and higher temperatures.

In addition to phosphoric acid, other acids, especially organophosphonic acids such as phenylphosphonic acids and akylphosphonic acids, have been tried as the dopants, with the aim of improving the acid retaining properties [25a]. Simple doping in a solution of these acids in solvents such as tetrahydrofuran (THF) and alcohols results in very low doping contents. High acid-doping levels have been reportedly achieved by using the TFA method.

Ünsal and Kiefer [132,133] used polyvinylphosphonic acid (PVPA) as the polyelectrolyte, immobilized in the PBI matrix by interpenetration, cross-linking and covalent bonding. The electrolyte is unlikely to be washed out when the membrane is exposed to a liquid. This is especially desirable for the liquid-fed direct methanol fuel cell (DMFC). Based on this type of membranes BASF-PEMEAS has developed an MEA product under the trade mark Celtec®-V. Being the simplest polymeric diprotic acids with highest density of immobilized phosphonic acid, PVPA

has been considered for PEMFC applications [134,135] and more interest has arisen recently [18]. Synthesis [136] and characterizations with respect to water content, self-condensation and proton conductivity as a function of relative humidity has recently been investigated [137].

2.3. Membrane modifications

The conductivity of PBI generally increases with increasing acid-doping level, i.e. acid content. At the same time the mechanical strength decreases with acid-doping level. The optimum doping level is thus a compromise between these two effects. Different methods are being explored to improve the proton conductivity without sacrificing mechanical strength or vice versa. The methods include ionic and covalent cross-linking of the polymer as well as preparation of composite membranes.

2.3.1. Ionic cross-linking

Flexible ionomer networks can be prepared from acid–base polymers by ionically cross-linking of polymeric acids and polymeric bases [138–142], as recently reviewed by Kerres [16]. Basic polymers are typically PBI, but other polymers such as poly(4-vinylpyridine) (P$_4$VP) [143], aminated PSF [144,145] and PEEK [146] and pyridine containing polymers [91,92] have also been used. The acidic polymers are typically sulphonated polysulphone (SPSF) [147,148], sulphonated polyetheretherketone (SPEEK) [149], sulphonated poly(2,6-dimethyl-1,4-phenylene oxide) (SPPO [150]), sulphonated poly(arylene thioether)s [151], and sulphonated poly[bis(phenoxy)phosphazene] (SPOP [152]). In addition perfluorosulphonic acid polymers, e.g. Nafion® was first coated with PBI by Hobson et al. [153] in order to reduce the methanol permeability. The work has inspired more interest in developing Nafion®-PBI blend membranes [154–156]. Improved durability at open circuit voltage (OCV) and at constant current density has been reported by Zhai et al. [156], however, the test was performed in a relatively short period of time (480–720 h).

When an acidic polymer and a basic polymer, preferably dissolved in a common solvent for membrane casting,

are mixed, precipitation of a polysalt occurs. To avoid this, the acidic polymer is usually prepared in a neutralized form, e.g. either mixed with a volatile base, typically diethyl amine or triethyl amine, or converted to the corresponding metal salt, for example, the sodium form of Nafion, which can be acidified after a homogeneous blend membrane has been prepared by solution casting.

Generally speaking, ionically cross-linked membranes suffer from poor thermal stability in aqueous media as the ionic cross-link breaks at higher temperatures [16], resulting in unacceptable swelling and therefore mechanical instability. On the other hand, covalently cross-linked membranes tend to become brittle as they dry out. Kerres and co-workers [157,158] recently introduced a covalent cross-linker (1,4-diiodobutane, DIB) into an ionically cross-linked blend. The resultant membrane was covalent-ionically cross-linked, showing high conductivity (above 0.1 S cm^{-1} as measured in 0.5N HCl), low swelling and good thermal stability.

Further doping of PBI-based acid–base blend membranes with phosphoric acid gives a ternary membrane [159,160]. Compared with acid-doped pure PBI membranes, this ternary membrane has improved mechanical strength, allowing for a higher acid-doping level and therefore high conductivity and better fuel cell performance. In this case another issue arises, being the chemical stability of the acidic polymers at elevated temperatures and in the presence of doping acids. Kerres et al. [161,162] have recently synthesized sulphonated partially fluorinated arylene main chain polymers (Scheme 9), showing excellent stability in hot phosphoric acid at temperatures up to 160 °C. Their blend membranes with PBI exhibit excellent thermal stability and extended stability. Phosphoric acid-doping levels as high as 11–12 have been achieved with high proton conductivities (above 0.1 S cm^{-1}), less acid swelling, reasonable mechanical strength and therefore better fuel cell performance [163].

2.3.2. Covalent cross-linking

Covalent cross-linking of polybenzimidazoles is well known. In a US Patent issued in 1977, Davis and Thomas
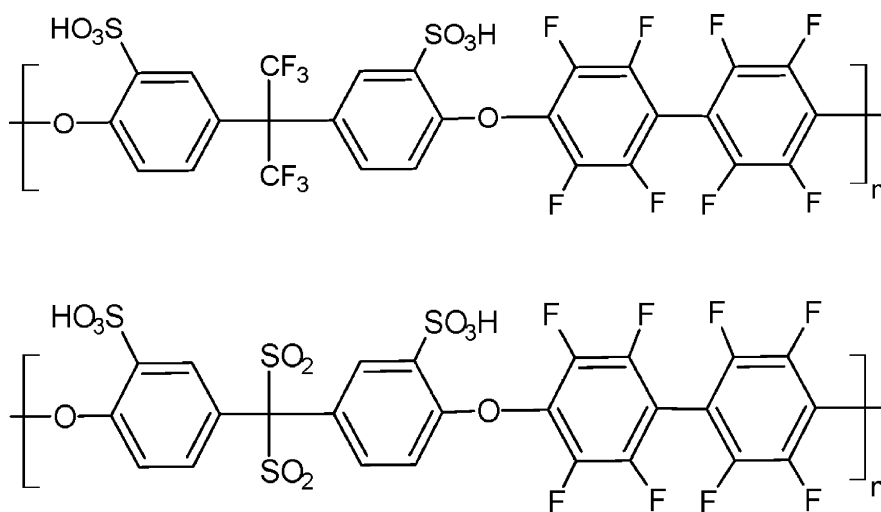
Scheme 9. Partially fluorinated sulphonated polymers used for preparation of acid–base blend membranes with PBI [163,164].

Table 1
PBI-based composite membranes.

Organic phase	Inorganic phase	Remarks	Ref.
PBI	$ZrP + H_3PO_4$	9×10^{-2} S cm^{-1} at 200 °C, 5% RH	[32]
	$PWA/SiWA + H_3PO_4$	$3–4 \times 10^{-2}$ S cm^{-1} at 200 °C, 5% RH	
PBI	$SiWA + SiO_2$	2.2×10^{-3} S cm^{-1} at 160 °C, 100% RH	[172,173]
PBI	$PWA + SiO_2 + H_3PO_4$	Thermally stable at <400 °C; 1.5×10^{-3} S cm^{-1} at 150 °C, 100% RH	[171]
PBI	Zr(PBTC)	3.8×10^{-3} S cm^{-1} at 200 °C, 100% RH	[176,177]
PBI-sPEEK	BPO_4	6×10^{-2} S cm^{-1} at RT	[174]
F_6-PBI	Modified MMT $+H_3PO_4$	Reduced thermal expansion and improved mechanical properties	[100]
PBI-PTFE	$+H_3PO_4$	ca. 22 μm membranes but low OCV	[179]
PBI-PTFE	$Sn_{0.95}Al_{0.05}P_2O_7-P_xO_y$	4 wt% PBI–10% PTFE, at 200 °C: 0.04 S cm^{-1}; fuel cell OCV 0.96 V, 284 mW cm^{-2}	[178]

[164] described that imidazole groups of the polybenzimidazole membrane can be cross-linked by an organic acid or its halide with two or more functional groups per molecule. In this way the polybenzimidazole is covalently cross-linked through an amide-type linkage. The cross-linked polybenzimidazole is tougher than non-cross-linked analogues and shows improved compaction resistance during prolonged usage at higher pressures. Different cross-linkers have been explored such as ethylene glycol diglycidyl ether (EGDE) [24b], terephthaldehyde (TPAH) [104], tetracarboxylic dianhydride (TCDA) [165], divinyl sulphone [166], α-dibromo-p-xylene (DBpX) [167,168], 3,4-dichloro-tetrahydro-thiophene-1,1-dioxide [169], dichloromethyl phosphonic acid [170], among many others.

For fuel cell applications, dibromo-p-xylene (DBpX) has been used as the cross-linker for PBI membranes cast from a DMAc solution [171]. After heat treatment at temperatures above 250 °C cross-linked membranes are obtained with improved mechanical strength. At an acid-doping level of 8.9 per repeat unit, the cross-linked PBI membrane has a similar mechanical strength as that of linear PBI at an acid-doping level of 6 per repeat unit, while the conductivity is almost doubled because of the high acid content. It is interesting that, when exposed to the Fenton test, e.g. a 3% hydrogen peroxide solution containing 4 ppm Fe^{2+} at 68 °C, the cross-linked polybenzimidazole membranes show little visible deterioration [171] (see Section 3.3).

2.3.3. Composite membranes

Inorganic–organic composites are the focus of recent attempts to develop proton exchange membranes [10–12]. Addition of a hygroscopic moiety (e.g. SiO_2) to an ionomer, for example, will increase the water retention and also make the materials stiffer. In case that the inorganic filler is a solid proton conductor such as zirconium phosphates or heteropolyacids, an improvement of the conductivity may also be seen. In addition to the mechanical and conducting properties, an inorganic component may assist in improving the thermal stability, water absorption, reactant crossover resistance, and other properties of the polymer membranes.

PBI and PBI blend composites have been prepared containing inorganic proton conductors including zirconium phosphate ($Zr(HPO_4)_2 \cdot nH_2O$, ZrP) [32], phosphotungstic acid ($H_3PW_{12}O_{40} \cdot nH_2O$, PWA) [172]; silicotungstic acid ($H_4SiW_{12}O_{40} \cdot nH_2O$, SiWA) [32,173,174], and boron phosphate (BPO_4) [175]. When further doped with phosphoric acid, high conductivity of 9.0×10^{-2} S cm^{-1} at 5% RH and 200 °C was obtained with PBI composite membranes [32].

Based on the hexafluoro PBI (F_6-PBI, see Scheme 5i) [99,100] and dodecylamine (DOA)-modified montmorillonite (MMT) [176], Chuang et al. [100] prepared nanocomposite membranes, showing reduced coefficient of thermal expansion, reduced methanol crossover, and much decreased plasticizing effect of the phosphoric acid after acid doping.

Pure solid inorganic proton conductors are brittle and therefore mechanically poor when used directly as membranes. A thermally stable polymer like PBI might be used as a binder to prepare composite membranes with improved mechanical strength, flexibility, and conductivity. Yamazaki et al. [177,178] prepared zirconium tricarboxybutylphosphonate ($Zr(O_3PC(CH_2)_3(COOH)_3)_2$, Zr(PBTC)) membranes with PBI as a binder. A composite membrane of 50% Zr(PBTC)-50%PBI showed a conductivity of 3.8×10^{-3} S cm^{-1} at 200 °C and under an equilibrium water vapour pressure of 1.38 MPa. Similarly, Heo et al. [179] fabricated composite membranes of $Sn_{0.95}Al_{0.05}P_2O_7$ with PBI and PTFE, showing improved conductivity and stability compared to the system without PBI.

Composite membranes of polytetrafluoroethylene (PTFE) and PFSA, e.g. Nafion are well known. Using the Nafion covered PTFE matrix where Nafion serves as a coupling agent via an acid–base reaction with PBI, Lin et al. [180] prepared PTFE-PBI composite membranes, followed by acid doping. Such a composite membrane can be made in small thickness with good mechanical strength. However, the low OCV indicated high gas permeability. These efforts are summarized in Table 1.

3. Structure and characterizations

3.1. Spectroscopic studies

The infrared (IR) [30,31,181–188], Raman spectroscopy [187–189] and nuclear magnetic resonance (NMR) spectra [181,182,186] have been made to investigate the polymer and its protonation by acids. For pristine PBI, the IR spectrum [183–185] from 2000 to 4000 cm^{-1} is of particular interest since most of the informative N–H stretching modes occur in this range, with typically three distinguishable bands at 3415, 3145 and 3063 cm^{-1}. According to Musto et al. [183], the relatively sharp peak centred at 3415 cm^{-1} is attributed to the stretching vibration of isolated, non-bonded "free" N–H groups, whereas the broad absorption band located around 3145 cm^{-1} is assigned to
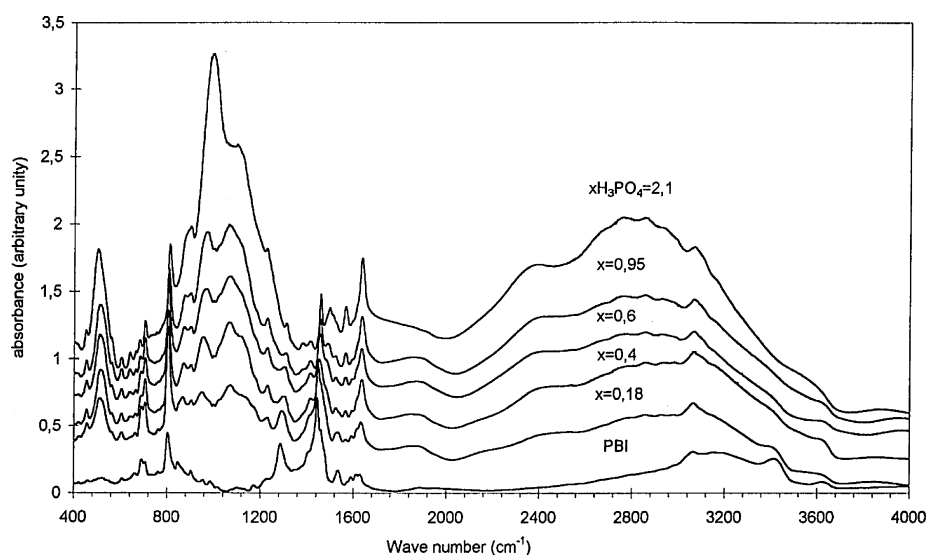
Fig. 3. Infrared spectra of PBI-xH$_3$PO$_4$ membranes [29] [reproduced from Bouchet and Siebert with permission of Elsevier Science Ltd.].

stretching vibrations of self-associated, hydrogen-bonded N$\cdots$H groups.

When PBI is doped with phosphoric acid, a very broad absorption band complex appears in the wave number range from about 2400 to 3000 cm^{-1}, corresponding to the protonation of the nitrogen of the imide by transferring one or more protons from H$_3$PO$_4$ to imidazole groups of PBI [29,30]. As the doping level increases, the intensity of this new band complex increases at the expense of the absorption of both the N–H groups at 3415 and the N–H$\cdots$H groups at 3145 cm^{-1}. The intensive absorption bands in the 400–1300 cm^{-1} spectral region are characteristic of the anions, predominantly H$_2$PO$_4^{-1}$. Bouchet and Siebert [29] found that the area of the peak at 1630 cm^{-1} is sensitive to the protonation and approaches the same value for all the acids after reaching the maximum degree of protonation (see Fig. 3).

PBI is amorphous, or at least with a very low extent of crystallinity, as revealed by X-rays diffraction patterns [34,93]. When doped with phosphoric acid, the residual crystalline order is completely lost as the acid has a plasticizing effect. This is indicated by the remarkable T_g decrease observed by Hughes et al. [182] using differential scanning calorimetry (DSC). When cast directly from a TFA solution, the membrane is of higher crystallinity, as reported by Litt et al. [34]. Heat treatment at above 200 °C lowers the crystallinity. The high crystallinity might be the reason for the observed high conductivity since the crystalline regions have low acid content, forcing the excess acid into the amorphous phase and increasing the overall conductivity [34]. Kim et al. [87] reported that quenching the directly cast p-PBI membrane immediately to −20 °C could also prohibit the formation of the crystallites.

Using ^{1}H and ^{31}P magic-angle spinning NMR, Hughes et al. [182] investigated the polymer–acid interaction. The assignment of the ^{1}H and ^{31}P resonances was made, showing the four different ^{31}P environments, i.e. bound and unbound phosphoric acid molecules (H$_3$PO$_4$) and acid anion (H$_2$PO$_4^-$), in good agreement with the IR obser-

vations [29]. This implies that the protonation of the imidazole rings occurred by the phosphoric acid together with hydrogen bonding of both H$_3$PO$_4$ and H$_2$PO$_4^-$.

Jayakody et al. [186] studied the mass-transport in both DMAc and PPA cast membranes by ^{1}H and ^{31}P NMR. At similar PA loading levels, the proton diffusivity is ascertained to be about an order of magnitude higher in the PPA-cast membranes than in DMAc-cast membranes, showing the significant effect of membrane processing on membrane transport properties. Phosphate counter-ion mobility was inferred to be more than 2 orders of magnitude lower than that of the protons, which supports a Grotthus-type mechanism of proton conduction.

Raman spectra of PBI [187–189] and acid-doped PBI [187,188] have been studied. The FT-Raman band at 1000 cm^{-1} was assigned to the *meta*-benzene ring vibration, unchanged after the acid doping. The band at 1570 cm^{-1} was found to correspond to the protonation of the imidazole ring [187]. By plotting the ratio of the band intensity of 1000 cm^{-1} to that of 1570 cm^{-1} against the acid-doping level, Voyiatzis [187] confirmed the maximum protonation of 2 for PBI by phosphoric acid.

3.2. Water uptake and acid doping

It is well known that PBI has a high affinity for moisture. By immersing a dry PBI membrane in distilled water at room temperature, up to 15–19 wt% of water can be absorbed, corresponding to about 3 water molecules per repeat unit of PBI. The water uptake is due to intermolecular hydrogen bonding between water and N and N–H groups in the PBI [188,189]. In case of acid-doped membranes at an acid-doping level of up to 2 mole H$_3$PO$_4$ per PBI unit, the water uptake is lower than that for the pristine PBI [188]. It seems that the active sites of the imidazole rings are preferably occupied by the acid molecules. At higher acid-doping levels, however, the water uptake is higher than that of pristine PBI membranes, indicating that this water uptake is associated with the doping acid. At acid-doping levels around 3 acid molecules per repeat unit, about 25% of the

measured membrane volume swelling is found to be due to the water uptake [188].

As discussed above, the infrared [29] and Raman [187] spectroscopic analysis suggests that the maximum degree of protonation of PBI by phosphoric acid is reached at a doping level of 2 acid molecules per repeat unit. This is confirmed by a gravimetric measurement [188]. Ma et al. [33] have estimated the equilibrium constant for the following reaction:

$$H_3PO_4 + PBI \leftrightarrow H_2PO_4^- + PBI\text{-}H^+ \tag{2}$$
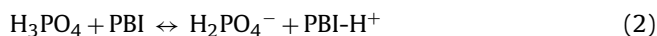
By using the dissociation constant of protonated 2-phenyl benzimidazole ($K^{PBI\text{-}H^+} = 5.9 \times 10^{-6} \text{ mol L}^{-1}$) and the first dissociation constant of phosphoric acid ($K^{a_1}_{H_3PO_4} = 6.9 \times 10^{-3} \text{ mol L}^{-1}$), they obtained the equilibrium constant $K = 1.17 \times 10^3$.

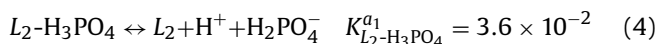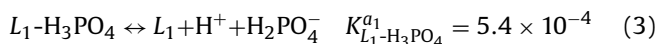He et al. [190] studied the doping chemistry of PBI membranes by the Scatchard method. By considering the distribution of phosphoric acid between the aqueous phase and the polymer immersed in the solution, a two linear segment plot of the ratio of the measured PBI doping level, $[L^T]_B$, to the doping acid concentration, C, a plot of $[L^T]_B/C$ against the measured PBI doping level, $[L^T]_B$ was obtained. It is confirmed that there are two types of polymer sites for the acid doping, one with higher affinity (site type L_1 with a complexation constant $K^1 = 12.7 \text{ L mol}^{-1}$), giving a maximum acid-doping level of 2, and the other with lower affinity (site type L_2 with complexation constant $K^2 = 0.19 \text{ L mol}^{-1}$). The dissociation constants for the complexing acid onto these two types of PBI sites are found to be

$$L_1\text{-}H_3PO_4 \leftrightarrow L_1 + H^+ + H_2PO_4^- \quad K^{a_1}_{L_1\text{-}H_3PO_4} = 5.4 \times 10^{-4} \tag{3}$$

$$L_2\text{-}H_3PO_4 \leftrightarrow L_2 + H^+ + H_2PO_4^- \quad K^{a_1}_{L_2\text{-}H_3PO_4} = 3.6 \times 10^{-2} \tag{4}$$

respectively, that is, about 10 times smaller than that of aqueous phosphoric acid in the first case but 5 times higher in the second. It is the acid bound onto the second type of PBI sites, with a larger dissociation constant, that contributes most of the proton conductivity of the acid-doped membranes.

3.3. Thermal and oxidative stability

The thermal stability of PBI has been extensively studied by thermogravimetric analysis (TGA) with mass spectrometry (MS) of the purge gas from the TGA [35,191,192]. For pristine PBI, typically about 10–15% weight loss occurs at temperatures up to 150 °C, due to absorbed water. From 150 to 500 °C, there is no further significant weight loss, indicating the excellent stability of PBI polymer samples. At temperatures over 500 °C, a significant weight loss occurs, accompanied by the formation of carbon dioxide. For the acid-doped PBI sample, weight losses due to dehydration of phosphoric acid and pyrophosphoric acid were observed. In the presence of platinum catalysts under atmosphere of either nitrogen, 5% hydrogen or air, Samms et al. [35] observed only weight losses due to water at temperatures below 400 °C, showing adequate thermal stability of this membrane for fuel cell applications.
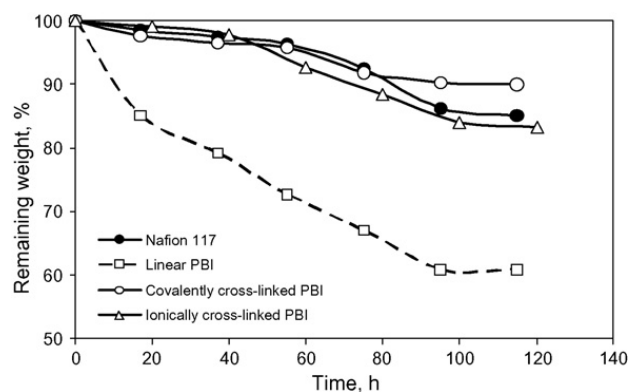

Fig. 4. Membrane degradation in 3% H_2O_2 containing 4 ppm Fe^{2+} at 68 °C. Solid lines indicate that the samples remained as a whole membrane, whereas dashed lines indicate that samples were broken into small pieces. Data for ionically cross-linked PBI were from [163] and the rest from [171].

Chemical stability of membranes is of much concern to the lifetime of PEMFC. In situ formed H_2O_2 and $^\bullet$OH or $^\bullet$OOH radicals from its decomposition are believed to attack the hydrogen containing bonds in polymer membranes. This is assumed to be the principal degradation mechanism of common PEMFC membranes. Experimentally, the generation of these radicals can be achieved by Fe^{2+}/Fe^{3+} catalysed H_2O_2 decomposition. Based on this method, the so-called Fenton test is used for the stability evaluation of PEMFC membranes [193]. In this connection it seems that membranes based on perfluorinated sulphonic acid, e.g. Nafion® exhibit better chemical stability than those based on polyaromatic hydrocarbons. And this peroxy radical attack would be much more aggressive at temperatures exceeding 100 °C.

By being exposed to a 3% hydrogen peroxide solution containing 4 ppm Fe^{2+} at 68 °C, PBI membranes have been evaluated by the weight loss and visual observation [163,170,171]. The PBI membrane was broken into small pieces after 30 min (indicated with the dashed lines in Fig. 4). After the first 20 h, the PBI membrane showed a weight loss of about 15%. As a comparison, Nafion 117 membranes have only 1% weight loss during the same period of time. It is shown by Gaudiana and Conley [194] that the initial stages of oxidative attack to benzimidazoles occur preferentially on the aromatic rings bearing the nitrogen function and subsequently the amine portion of the molecules. That is to say, the weak link is the nitrogen containing heterocyclic and adjacent benzenoid rings.

It is interesting that cross-linking of PBI can be achieved by an amide-type linkage through imidazole rings of the polymer. The cross-linking has proved to be an effective way to improve the stability of the aromatic heterocyclic polymers. As seen from Fig. 4, both ionically cross-linked [163] and covalently cross-linked [171] PBI membranes remained in a good membrane form even after 118 h (indicated with solid lines). After the first 20 h, about 2% of weight loss was observed for the cross-linked PBI membranes. Over the whole 120 h period of the test, the cross-linked PBI membranes behave in a comparable way to Nafion 117 membranes.
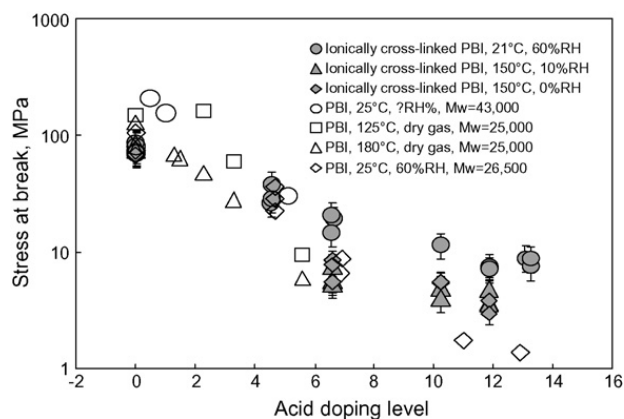
Fig. 5. Tensile strength of DMAc-cast PBI membranes as a function of acid-doping level at different temperatures. RH is relative humidity. The tensile strength is with respect to the initial dimensions of samples. Data for ionically cross-linked PBI were from [163]. Data for M_W = 43,000 PBI were from [34]. Data for M_W = 25,000 PBI were from [195].

3.4. Mechanical strength

The strong hydrogen bonding between $-N=$ and $-NH-$ groups in PBI is the dominant molecular force, resulting in close chain packing and therefore good mechanical strength of membranes. The dry PBI membrane has a small elongation at break of around 1–3%, and an intermediate tensile strength of about 60–70 MPa at room temperature. When saturated with water, the elongation and tensile strength increase to about 7–10% and 100–160 MPa, respectively [14].

When phosphoric acid is introduced into the polymer structure at a low acid-doping level range, say, below 2, the molecular cohesion between the PBI chains is decreased. However, the hydrogen bonding between nitrogen atoms and phosphoric acid increases the cohesion. As a result of these opposite effects, no significant change of modulus or tensile strength of the PBI membranes is observed [34]. With acid-doping levels higher than 2, i.e. when the number of acid molecules surpasses the number of the basic sites, free acid will be present. The free acid would increase the separation for PBI backbones and therefore decrease intermolecular forces. Consequently the membrane strength is decreased dramatically, more at higher temperatures, as shown in Fig. 5. The strength is also strongly influenced by the average molecular weight. In a range from 20,000 to 55,000 g mol^{-1}, the tensile strength of acid-doped PBI membranes is found to increase from 4 to 12 MPa [195].

The selection of a practical acid-doping level should take into account both conductivity and mechanical strength, which are opposite functions of the doping level. For thin DMAc-cast membranes, a useful doping level around 5–6 mol of H_3PO_4 per PBI unit has been suggested [14]. This practical acid-doping level range seems also valid for TFA-cast membranes to some extent. When cross-linked, the PBI membranes show much improved mechanical strength, especially after acid-doping [163,171]. As a consequence, the acid-doping level can be extended to a higher range of 10–13, still with sufficient mechanical strength of the

membranes (see Fig. 5). This will in turn give a higher conductivity.

The PPA-cast membranes, however, behave differently mechanically. It is reported that at an acid-doping level of 20–40 mol phosphoric acid per repeat unit, the PPA-cast membranes still exhibit rather high tensile strength, from 1 to 3.5 MPa [88,89]. It should also be remarked that the polymer used for preparing the PPA membranes had very high IV or molecular weights, which is known to have significant effect on mechanical strength of membranes.

4. Electrochemical and transport properties

4.1. Proton conductivity

The proton conductivity of PBI was first studied more than 30 years ago [196,197], though under poorly defined conditions. For phosphoric acid-doped PBI membranes, the proton conductivity has been measured by several groups. Fontanella et al. [131] measured the conductivity of acid-doped PBI at compressions of up to 0.25 GPa. At room temperature the conductivity decreases with increasing pressure for both acid-doped PBI and 85% phosphoric acid, as expected due to the viscosity increase. From the slopes of the logarithmic conductivity versus pressure curves the activation volume of acid-doped PBI was estimated and found to be much larger than that of 85% aqueous PA but similar to that of PFSA membranes. This is an indication that the acid-doped PBI is a single-phase polymer electrolyte where ion transport is similarly mediated by segmental motions of the polymer, presumably the pedant side chains in case of PFSA membranes [198].

Bouchet and Siebert [29,199] studied anhydrous conductivity of different acid-doped PBI systems, and proposed an activated mechanism for the proton migration. They suggested that the proton migrates from an imide site to a neighbouring vacant one, and this migration is assisted by the counter anion with a Grotthus mechanism. The ^1H and ^{31}P NMR showed that phosphate counter-ion mobility was more than 2 orders of magnitude lower than that of the protons [186], supporting also the Grotthus mechanism of proton conduction in the membranes. This seems to be consistent with the unreported transference number measurements, done by one of the authors' group, where the cation transference number (t^+) is found to be 0.98 [200].

Spectroscopic studies revealed the existence of bound and unbound phosphoric acid molecules (H_3PO_4) and acid anion ($H_2PO_4^-$) in acid-doped PBI membranes [182]. From a proton conducting point of view, the bound acid molecules and acidic anions contribute to the proton conductivity only via the Grotthus mechanism, whereas the presence of unbound $H_2PO_4^-$ ions is essential for the vehicle mechanism, but participates as well in the Grotthus mechanism. In addition the hydrogen bonding between free H_3PO_4 has been observed, which would be a prerequisite for the Grotthus mechanism.

The conductivity of phosphoric acid-doped PBI membranes has been measured at different acid-doping levels. Different acid-doping levels attribute to different mechanisms of proton transfer, i.e. along different chains of proton

donors and acceptors. Ma et al. [33] proposed the order of the rate of proton transfer between various species: H_3PO_4 to H_2O > H_3PO_4 to $H_2PO_4^-$ > N–H^+ to $H_2PO_4^($ > N–H^+ to H_2O > N–H^+ to N–H.

At an acid-doping level of lower than 2 virtually all acid molecules are believed to donate a proton to the unprotonated N-site and to be bounded to the polymer matrix. In this case, proton exchange most likely happens between protonated and non-protonated imino nitrogen groups on neighbouring polymer chains. Bouchet and Siebert [29] reported that the conductivity is about 10^{-7} S cm^{-1} for dry PBI with an acid-doping level of 2 at 30 °C. Kawahara et al. [31] measured the conductivity of PBI with an acid-doping level of 1.9 from room temperature to 160 °C, being in a range of 10^{-9} to 10^{-5} S cm^{-1} under anhydrous states. Even under humidified atmosphere and at 200 °C, the conductivity at this low acid-doping level was found to be lower than 10^{-2} S cm^{-1} [32]. These findings indicate that high conductivity is only obtainable with free acid, i.e. at acid-doping levels higher than 2.

At high acid-doping levels, in a range of 4–6, the proton migration is proposed to happen mainly along the acid and anion chain ($H_2PO_4^-$–H^+–$H_2PO_4^-$) or the acid and H_2O ($H_2PO_4^-$–$H^+\cdots H_2O$) chain depending on the water content [33]. In this case, the conductivity mechanism would be similar to that of a concentrated H_3PO_4 solution. The measured conductivity is about 4-7 × 10^{-2} S cm^{-1} at 200 °C, indicating that the presence of molecular acid contributes the major part of the conductivity [32,33].

Fig. 6 summarizes the conductivities of different types of PBI membranes doped at different acid levels. The conductivity of the TFA-cast membranes was measured under a constant relative humidity (varied water-to-air ratio) [33], while that of the DMAc-cast membranes was obtained under a constant water-to-air ratio [32]. They are only comparable at temperatures close to 200 °C. It can be seen that the TFA-cast membranes exhibit slightly higher conductivity. With cross-linked membranes higher acid-doping
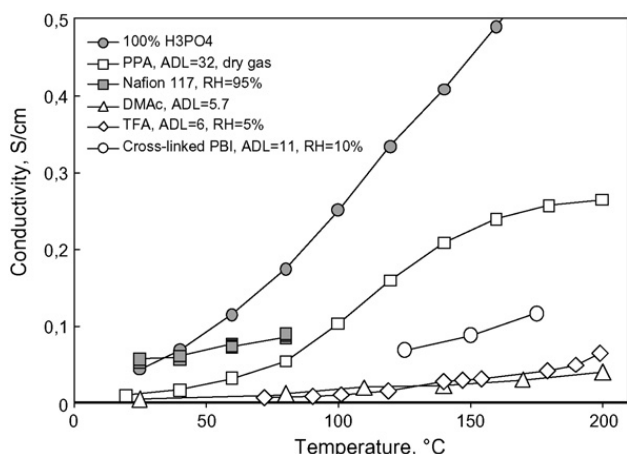
levels of 10–12 can be used, giving conductivities around 0.1 S cm^{-1} [163].

The membrane processing and morphology have also significant effects on the proton transport and conductivity. The NMR study by Jayakody et al. [186] showed that the proton diffusivity is about an order of magnitude higher in the PPA-cast membranes than in DMAc-cast membranes. Apparently an additional proton transport mechanism exists involving rapid exchange between the phosphoric acid and pyrophosphoric acid species. At an acid-doping level of 32, corresponding to 91 wt% phosphoric acid and 9 wt% PBI, the PPA-cast membranes exhibit a conductivity as high as 0.26 S cm^{-1} at 200 °C under dry conditions, as seen from Fig. 6 [89]. This conductivity is, however, still much lower than that of 100% phosphoric acid. Apart from the effective dilution cause by the polymer, it is likely that the H-bond structures present in pure H_3PO_4 are broken by the polymer, making proton jumping and perhaps also acid molecule movement more difficult. Similar effects were observed when small molecules such as imidazole and 1-methyl imidazole were introduced into concentrated phosphoric acid instead of water [201].

4.2. Electro-osmotic water drag and methanol crossover

The electro-osmotic drag coefficient is defined as the number of water molecules moved with each proton in the absence of a concentration gradient [202]. This coefficient has been determined previously for Nafion membranes and a coefficient of 2.5–3.0 H_2O/H^+ has been reported for liquid water-equilibrated Nafion membranes at room temperature [203,204]. When equilibrated with high relative humidity vapour, the drag coefficient was found to be in a range from 0.9 to 3.2 at room temperature. Under fuel cell operating conditions, especially at higher temperatures and equilibrated with a water–methanol mixture, this value was found to be even higher [205]. The large water drag coefficients for Nafion are resulting from its relatively large water-filled domains and the vehicle mechanism of proton conductivity, i.e. via hydration species like H_3O^+, $H_5O_2^+$, or $H_9O_4^+$, etc. For proton conduction entirely by the Grotthus mechanism, one would expect an electro-osmotic drag coefficient of zero, because proton transport occurs without a net water transport [206]. For acid-doped PBI membranes, it was found that the electro-osmotic drag coefficient of water is nearly zero [207,208].

It has been suggested that materials with a low electro-osmotic drag may offer the potential for improved selectivity in DMFCs [209]. Because methanol and water are completely miscible, it is unlikely that high selectivity can be achieved in polymers with large water domains. For PBI membranes, the electro-osmotic drag coefficient of methanol was found to be essentially zero [207]. Similar results of the methanol crossover rate were obtained by a methanol sorption/permeation method [21] and a real-time spectrometric analysis of the cathode exhaust stream of a fuel cell operating with a current [210], indicating little contribution of the electro-osmotic drag mechanism. For PBI membranes doped with 5 mol H_3PO_4 per repeat unit at 150 °C and 50/50 water/methanol vapour, the methanol crossover was found to be corresponding

Fig. 6. Proton conductivity of 100% phosphoric acid, Nafion 117, and different types of acid-doped PBI membranes. The PPA-cast membrane was with an acid-doping level of 32 and at relative humidity of 0% [89]. The DMAc-cast membrane was with an acid-doping level of 5.7 and under atmosphere with a water-to-air molar ratio of about 0.7 [32]. The TFA membrane was with an acid-doping level of 6.0 and at relative humidity of 5% [33]. Data for cross-linked PBI, 100% PA and Nafion were from [163].

Table 2
Methanol crossover rates.

Methods and conditions	Report results	Ref.
Sorption/permeation method, PBI-5H$_3$PO$_4$, 150 °C, 90/10 water/methanol vapour	1.5×10^{-6} cm^2 s^{-1} bar^{-1}	[21]
Real-time fuel cell, PBI-5H$_3$PO$_4$, 150 °C, water/methanol vapour, 90 μm	<10 mA cm^{-2} (ca. 6×10^{-6} cm^2 s^{-1} bar^{-1})	[2]
Real-time fuel cell, 90 °C, 1 M MeOH		
Celtec®-V, 120 μm	109 mA cm^{-2} (ca. 9×10^{-8} cm^2 s^{-1})	[133]
Nafion 117, 213 μm	240 mA cm^{-2} (ca. 3.6×10^{-7} cm^2 s^{-1})	
Diffusion cell, 1 M MeOH (liquid), RT		
Undoped PBI	8.3×10^{-9} cm^2 s^{-1}	[209]
Nafion 117	2.3×10^{-6} cm^2 s^{-1}	
Diffusion cell, 6 M MeOH (liquid), RT		
Undoped PBI	1.5×10^{-9} cm^2 s^{-1}	[114]
S-PBI	2.5×10^{-6} cm^2 s^{-1}	
Undoped PBI	1.5×10^{-8} cm^2 s^{-1}	[211]
N-substituted PBI	6×10^{-8} cm^2 s^{-1}	
Diffusion cell, 1.8 M MeOH, RT		
Hexafluoro(F$_6$)-PBI	2.8×10^{-8} cm^2 s^{-1}	
F$_6$-PBI-5%MMT	6×10^{-9} cm^2 s^{-1}	[100]
Nafion	3×10^{-7} cm^2 s^{-1}	
Diffusion cell, 1 M MeOH, 60 °C		
SPOP-12%PBI	1×10^{-7} cm^2 s^{-1}	[152]
Nafion	3.5×10^{-6} cm^2 s^{-1}	

to less than 10 mA cm^{-2} for a 100 μm thick membrane [21,210], equivalent to a methanol crossover rate of about 10^{-10} mol cm^{-1} s^{-1} bar^{-1}. Similar real-time measurements with Celtec®-V membranes based on PBI and PVPA were made by Gubler et al. [133] and showed, however, 10 times higher methanol crossover rate for a liquid fed 1 M methanol solution at 90 °C.

Methanol permeation measurements were reported using a diffusion cell with a liquid methanol solution as feed at the source side of the separating membrane and pure water in the receiving chamber at the other side [95,203,205,206]. This is a simple method to determine the methanol permeability via diffusion, which would be the dominating mechanism in case of a zero electric-osmotic drag coefficient for PBI membranes. As listed in Table 2, the results show a degree of scatter, even from the same research group [114,211]. It seems that undoped PBI membranes exhibit a methanol crossover rate of about 10^{-10} mol cm^{-1} s^{-1} at room temperature, as compared to 10^{-8} mol cm^{-1} s^{-1} for Nafion 117 membranes. These results provide an indication of methanol permeability of the base polymer, but are not relevant to fuel cell operation since doping with phosphoric acid is necessary to achieve conductivity, and thus are not compatible with liquid fed methanol solution.

4.3. Solubility, diffusion and permeability of gases

As the polymer electrolyte membrane is acting as a separator in a fuel cell, the gas permeability of the polymer is of particularly importance. In general hydrogen has a higher permeation rate than that of oxygen because of its smaller molecular size. Nafion membranes, for example, have low gas permeability for both hydrogen and oxygen. For dry membranes at 80 °C, Broka and Ekdunge [212] reported the results in a range of 10^{-11} to 10^{-12} mol cm^{-1} s^{-1} bar^{-1}.

As a glassy polymer PBI membranes are dense with close chain packing (density of 1.34 g cm^{-3} [213]), due to the rigidity of the structure and strong effect of hydrogen bonding. Very low gas permeability has been reported for PBI membranes [70], i.e. 2×10^{-13} and 5×10^{-15} mol cm^{-1} s^{-1} bar^{-1} for hydrogen and oxygen, respectively, at room temperature. At elevated temperatures from 80 to 180 °C, He et al. [195] reported a hydrogen permeability of $1.6-4.3 \times 10^{-12}$ mol cm^{-1} s^{-1} bar^{-1} and an oxygen permeability of $5-10 \times 10^{-14}$ mol cm^{-1} s^{-1} bar^{-1}. Pesiri et al. [69] reported a similar value (2.7×10^{-12} mol cm^{-1} s^{-1} bar^{-1}) for hydrogen at 180 °C.

When doped with acid, the membrane is swollen. At an acid-doping level of 6, for example, a volume swelling by 100–110% has been observed [195], resulting in a significant separation of the polymer backbones. As a result, the permeability of hydrogen and oxygen increases by 2–3 orders of magnitude in the temperature range from 80 to 180 °C, compared with the pristine PBI membranes, as shown in Fig. 7 [195]. This hydrogen permeability of acid-doped PBI membranes is confirmed by an electrochemical stripping current in a real fuel cell, which corresponds to $2-2.5 \times 10^{-10}$ mol cm^{-1} s^{-1} bar^{-1} [214].

In addition, the solubility coefficients, defined as C/p, where C is the gas concentration in the polymer and p is the applied gas pressure, were found to be 1.6×10^{-5} mol cm^{-3} bar^{-1} for hydrogen and 1.9×10^{-5} mol cm^{-3} bar^{-1} for oxygen in PBI membranes [70]. In the low range of solubility or gas pressure, Henry's law applies. Assuming to be a constant over the pressure range, the diffusion coefficient can be calculated from the permeability and solubility coefficients. For oxygen in PBI membranes this was found to be 3×10^{-10} cm^2 s^{-1}.

For acid-doped PBI membranes, electrochemical techniques have been used for determining the solubility
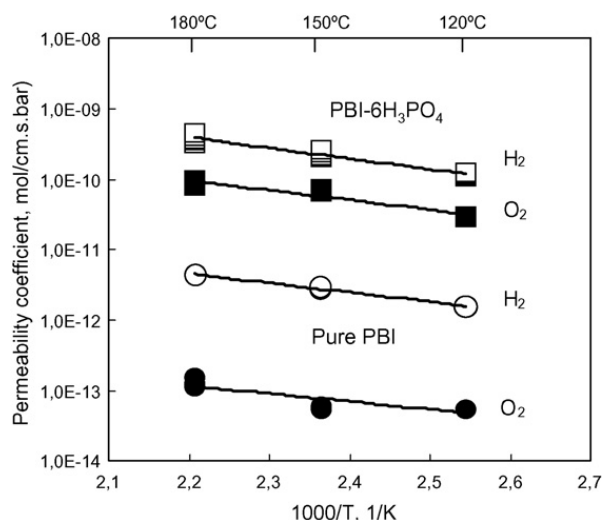
Fig. 7. Hydrogen (open) and oxygen (solid) permeability at different temperatures for PBI membranes before (cycles) and after (squares) being doped with phosphoric acid [195] [reproduced from He et al. with permission of Elsevier Science Ltd.].

and diffusion coefficients of oxygen. For PBI membranes doped with 6 H_3PO_4 per repeat unit at 150 °C under 10% RH, the solubility coefficient was found to be 6.8×10^{-7} mol cm^{-3} bar^{-1} and the diffusion coefficient was 3.2×10^{-6} cm^2 s^{-1} [215]. The diffusion coefficient seems consistent with diffusion in a mixture of pure phosphoric acid under these conditions (1.7×10^{-7} cm^2 s^{-1}) and a second phase where diffusion does not occur. On the other hand, the oxygen solubility coefficient is about four times higher than expected for pure phosphoric acid under these conditions [215].

4.4. Kinetics of oxygen reduction

It is well known that concentrated phosphoric acid imposes slow kinetics for oxygen reduction on the cathode due to the strong adsorption effect of anions onto the active sites of catalysts as well as the low solubility and diffusivity of oxygen. Zecevic et al. [216] studied the oxygen reduction kinetics at the Pt/PBI–H_3PO_4 interface by a rotating disk electrode covered with a thin PBI film, in 0.1 M aqueous acid solutions. Liu et al. [215,217] developed a micro band electrode technique that allows simulation of the catalyst/electrolyte interface under fuel cell-type operating conditions. It was found that both the kinetic and mass transport parameters in the Pt/PBI–H_3PO_4 system are comparable to those in the Pt/H_3PO_4 system under similar conditions. It seems that it is the amorphous H_3PO_4 that functions as the electrolyte, in which the oxygen molecules are mainly dissolved and through which the dissolved oxygen diffuses.

The cathodic oxygen reduction reaction (ORR) and anodic hydrogen oxidation reaction (HOR) kinetics on Pt-based catalysts in real PBI-based fuel cells have been studied [214,218]. With Pt-Ni/C as cathode catalysts, Neyerlin et al. [214] observed a significant decrease in the exchange current density (from 8.2×10^{-7} to 4–5×10^{-9} A cm^{-2}$_{Pt}$) for the ORR in acid-doped PBI membranes at 160 °C, compared with a Nafion cell at 80 °C. This

value is close to 2.2×10^{-9} A cm^{-2}$_{Pt}$ reported by Liu et al. [215] for oxygen reduction on a Pt/C catalyst in acid-doped PBI membranes at 150 °C, attributable to the presence of $H_2PO_4^-$ anion.

In the early research on PAFC, alternative electrolytes have been extensively investigated [219–222]. Some perfluorinated acids are found to be able to enhance the kinetics but suffer from low conductivity in concentrated solutions, high vapour pressure, and flooding the PTFE bonded gas diffusion electrodes. The possibility of using these perfluorinated acids or salts as additives in the PBI–H_3PO_4 system has not been explored in details, though some preliminary results look promising [223].

To summarize the discussion Table 3 lists properties of PBI membranes together with those of Nafion as a reference [209,224]. Data are primarily based on DMAc membranes from the author groups unless otherwise specified.

5. Fuel cell technologies

5.1. Catalysts, gas diffusion electrodes and membrane–electrode assemblies

Similar to low temperature PEMFC and PAFC, noble metals, i.e. platinum and its alloys are exclusively used as catalysts in PBI-based fuel cells. High surface area carbon blacks (e.g. Vulcan-XC 72 and Ketjen black) have been widely used as the catalyst support, though it is well known from the PAFC research that corrosion rates of these carbon materials are unacceptably high, as to be discussed in Section 5.5.3.

Limited independent work on the fabrication of gas diffusion electrodes has been reported compared with PAFC or Nafion-based PEMFC. Gas diffusion electrodes specific for high temperature PEMFC (>95 °C), most likely for acid-doped PBI membranes, are commercially available from BASF E-TEK (products HT250EW and HT140EW [225]), however, little technical information is available.

In the earlier works to develop PBI cells, Wang et al. [36] used PAFC electrodes treated by impregnation with the PBI polymer. The group also applied platinum black and platinum–ruthenium alloy for the manufacturing of cathodes and anodes by a filtering–pressing method, at a rather high loading of noble metal catalysts (4 mg cm^{-2}) for DMFC [226]. Although catalyst layer thickness and loading were investigated, electrode optimization was not thoroughly studied.

In general, PAFC electrodes are made with polytetrafluoroethylene (PTFE) as binder to make the catalyst layer hydrophobic and therefore allow both liquid acid and reactant gases to access the active sites of the catalyst. In this way a network structure of a three-phase zone is established, consisting of a proton conducting electrolyte, electron conducting catalysts, and reactant gases. For PEMFC electrodes, the key issue is to improve the protonic access to the majority of catalyst sites not in intimate contact with the membrane. This can be accomplished either by impregnating the PTFE bonded electrodes with an ionomer or using the ionomer as the binder.

Table 3
Properties of PBI membranes (DMAc-cast) before and after acid doping. Data were from author groups unless otherwise specified.

	Pristine PBI	PBI - 5 H_3PO_4	Nafion 117
Water uptake (mol H_2O/repeat unit)	~3	~3	22
Water swelling (vol%)	~25	~25	34
Conductivity (S cm^{-1}) (at 25 °C)	~0	~0.001 (25 °C)	0.04 (25 °C)
		~0.06 (180 °C)	0.1 (80 °C)
H_2 permeability ($\times 10^{12}$ mol cm^{-1} s^{-1} bar^{-1})	0.2 (20 °C) [70]	–	20 (25 °C)
	1.6 (80 °C)	120 (80 °C)	–
	2.7 [69]/4.3 (180 °C)	380 (180 °C)	–
O_2 permeability ($\times 10^{14}$ mol cm^{-1} s^{-1} bar^{-1})	0.5 [70] (20 °C)	–	10 (25 °C)
	5 (80 °C)	30 (80 °C)	–
	10 (180 °C)	90 (180 °C)	–
Solubility coefficient of O_2 ($\times 10^5$ mol cm^{-3} bar^{-1})	1.9 (25 °C) [70] (at 20 bar)	0.07 [215]	0.93 (30 °C)[224]
			0.44 (80 °C)[224]
Diffusion coefficient of O_2 ($\times 10^6$ cm^2 s^{-1})	0.0003 [70] (at 20 bar)	3.2 [215]	1×10^{-6} (30 °C) [224]
		(PBI-6PA, 150 °C, 10%RH)	8.7×10^{-6} (80 °C) [224]
Methanol crossover rate: vapour phase ($\times 10^9$ mol cm^{-1} s^{-1} bar^{-1})	–	<0.1 (150 °C) [210]	–
Liquid phase (1 M solution, cm^2 s^{-1})	8 (RT) [209]	–	60 (RT) [209]
Electro-osmotic drag coefficient of water (mol H_2O/H^+)	–	~0	~3.2
Tensile strength at break (MPa)	120–160 (21 °C, <2% RH)	25 (21 °C, <5% RH)	18 (25 °C)
	55 (150 °C, 6.6% RH)	4 (150 °C, 6.6% RH)	–
Elongation (%)	3 (21 °C, <2% RH)	40 (21 °C, <5% RH)	120 (25 °C)
	13 (150 °C, 6.6% RH)	86 (150 °C, 6.6% RH)	–
Thermal stability (°C) (decomposition in air, 5 °C/min)	>500	>500	>280
Oxidative degradation (%)	15 (broke into pieces)		
Weight loss after 18 h in 3% H_2O_2 + 4 ppm Fe^{2+} at 68 °C	<2 (cross-linked)	–	<1
Crease-crack resistance (ability to withstand 5-fold after drying)	–	Passed	Passed

For PBI cells, the used ionomers include PBI [227–230] or PBI–polyvinylidene difluoride (PVDF) [231] blend with subsequent acid doping, sulphonated polymer, e.g. Nafion [232] which in combination with phosphoric acid has proton conductivity at higher temperatures [233,234], or other polymers [235] that are containing functional groups for incorporating phosphoric acid. Different types of solvents, i.e. acetone and DMAc have been evaluated to prepare catalyst inks for the electrode casting [236].

The loading of the ionomer in the catalyst layer should be optimized by taking into account both ionic conductivity and the catalytic activity. High ionomer loading leads to high protonic conductivity, however, more catalytic sites will be covered by the ionomer and therefore have no access to the reactant gases. In the early work by the authors' group, using catalysts composed of 20 wt% Pt on carbon (Pt/C), the weight ratio of Pt to PBI loadings in the catalyst layer was about 0.7 [37,208,228]. Similar ratios were reported elsewhere, e.g. 0.6 by Kim et al. [232] and 1.0 by Seland et al. [227]. An investigation of PBI content used as the ionomer in the catalyst layer was recently made by Kim et al. [128,87]. They found that the ionomer to Pt/C ratio of 0.2 in the cathode gave best fuel cell performance. However, the catalyst composition, i.e. the Pt/C ratio was not specified in the study. As suggested by Seland et al. [227] in their study with catalysts of different Pt/C ratios, the ionomer loading in the catalyst layer should be optimized according to the surface area or the specific volume of the catalyst powder, since it is the carbon black that comprises the major volume of the catalyst layer [163].

A spraying method was developed using an ink of catalyst particles dispersed in a PBI solution in DMAc [227]. A mixture of Pt/C and PBI solution in NMP has been used for spraying and tape-casting [229,230]. For the purpose of tape-casting [224], a stiff gas diffusion layer (GDL) material was used with a supporting layer of PTFE bonded carbon black to smooth the surface. Effects of the electrode porosity, tailored by introducing various porogens, have been studied [228]. In general the tape-casting method is more demanding for a catalyst ink with higher viscosities, which is difficult to achieve at low ionomer loading without other additives.

In general, membrane–electrode assemblies (MEA) are fabricated by hot pressing the prepared electrodes onto the membrane. The primary challenge in preparing MEAs is to achieve good contact between the membrane, catalyst layer and GDL in order to maximize catalyst utilization during cell operation. An integral MEA structure is also essential to obtain long-term operation. The hot-pressing is usually performed at the softening temperature of the ionomer, typically 150 °C for PBI [14] and 200 °C for cross-linked PBI membranes [163].

5.2. Fuel cell performance

With H_2 as fuel, PBI cells have been demonstrated with operation on dry gases, i.e. without humidification for either hydrogen or air. Since the membrane conductivity increases with increasing the atmospheric humidity, it is expected that the cell performance might be further
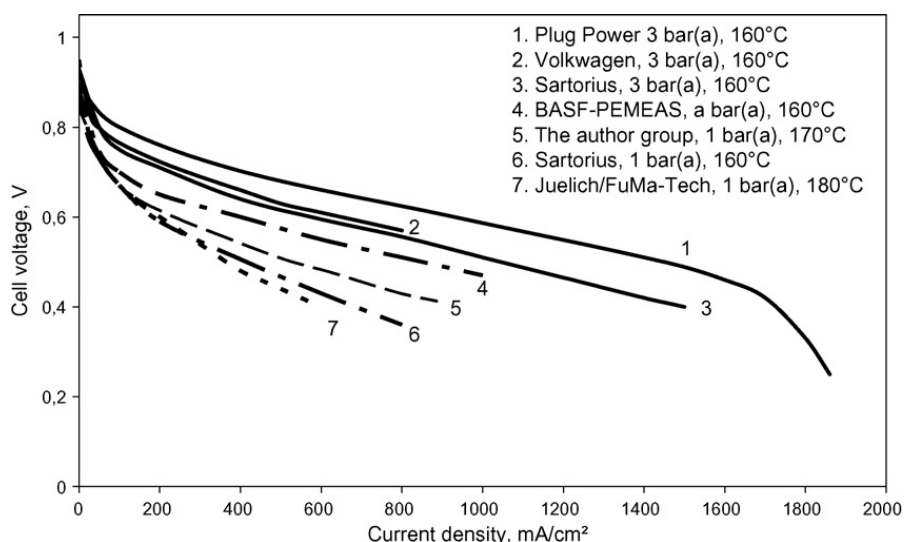
Fig. 8. Polarization curves of PBI cells operating with hydrogen and air at 160–180 °C. Solid lines are at a pressure of 3 bar absolute. Dashed and dotted lives are at a pressure of 1 bar absolute. The results by one of the authors' groups were an average of 44 MEAs of 256 cm^2 working area using cross-linked PBI membranes at an acid-doping level of 11 mol PA [163]. The PEMEAS (now BASF) [51] and PlugPower [238] results were based on PPA membranes. The Sartorius [239] result was based on post-doped membrane. The Juelich/FuMa-tech result [240] was achieved using cross-linked AB-PBI membranes. The Volkswagen result was achieved at a 15 cell stack with an active area of 200 cm^2 based on their own membranes [253].

improved if the fuel or the air is humidified to some extent, of course, at the expense of dilution effect. Jalani et al. [237] found, however, that humidification of anode fuel at temperatures (dew points) from 40 to 80 °C gives slightly poorer performance.

Fig. 8 shows a set of polarization curves of PBI cells operating with hydrogen and air at typically 160–180 °C, achieved by different groups. The solid lines are performances obtained under pressure of 3 bar absolute and dashed and dotted lines are from operation at ambient pressure. The results by one of the authors' group were based on cross-linked PBI membranes at an acid-doping level around 11, under ambient pressure. The electrodes of active area of 256 cm^2 were prepared from 50% Pt/C catalysts with a platinum loading of 0.6–0.7 mg cm^{-2}. The plot is an average performance at 170 °C of all together 44 MEAs.

Both PEMEAS (now BASF) [51] and PlugPower [238] cells were using the PPA membranes, which in general contain high acid content and therefore exhibit high proton conductivity. This can be seen from the smaller slopes of the voltage–current density curves in Fig. 8. The results by Sartorius were obtained by using the post-doped PBI membranes [239]. Stolten et al. [240] used cross-linked AB-PBI membranes from Fumatech. Unfortunately little information about catalysts and noble metal loadings is available.

At a cell pressure of 3 bar absolute (solid lines), Plug-Power reported a performance of 960 mA cm^{-2} at 0.6 V, based on PPA membranes. Volkswagen [253] and Sartorius [239] reported similar performance of about 600 mA cm^{-2} at 0.6 V. It should be remarked that the Volkswagen result was achieved at a 15 cell stack with an active area of 200 cm^2. For single cell tests, a much higher performance has been reported based on the so-called advanced PBI membranes. Under a pressure of 3 bar absolute and at a cell voltage of 0.6 V, the single cell power density as high as 0.8 W cm^{-2} at 160 °C and 0.12 W cm^{-2} at 40 °C has been

claimed [253], corresponding to a current density of 1300 and 200 mA cm^{-2}, respectively.

Direct use of methanol as fuel in a PBI cell is of special interest, since a much lower methanol crossover rate has been reported. Earlier tests of direct methanol fuel cells [226] showed, however, that the effect of the methanol crossover on the cathode performance is still significant, due to both the mixing potential effect and the poisoning effect of methanol on the cathode catalyst. Nevertheless, an open circuit voltage around 0.6–0.7 V and a peak power of more than 0.2 W cm^{-2} have been achieved at 200 °C under atmospheric pressure. Ünsal et al. [126,127] operated a DMFC using the commercial Celtec®-V MEA based on PBI-PVPA membranes, showing higher OCV and better fuel cell performance than Nafion 117 at methanol concentrations above 1 M. Other types of fuels, for example, ethanol, 1-propanol, 2-propanol [241], trimethoxymethane [242] and formic acid [243] have also been investigated.

5.3. Poisoning effect of CO and sulphur

Hydrogen produced by reforming of carbon containing fuels always contains traces of carbon monoxide (CO). When CO is present in the fuel stream, it competes with hydrogen for adsorption on the available sites of the catalyst surface. With the acid-doped PBI electrolytes, the CO poisoning effect has been examined [37]. The transient effect of CO poisoning was modelled and validated with experimental measurements [244].

Using a simple ratio of the poisoned H$_2$ oxidation current to the pure H$_2$ oxidation current, the relative activity of the catalysts for hydrogen oxidation at the presence of CO was estimated as a function of temperature and CO concentration [37], as shown in Fig. 9. The relative activity of the platinum catalyst for 20 ppm CO at 55 °C is about 24% [245], close to that for 100 ppm CO at 80 °C (23%) [246,247] or that for 1% CO at 125 °C (22%). A relative activity around
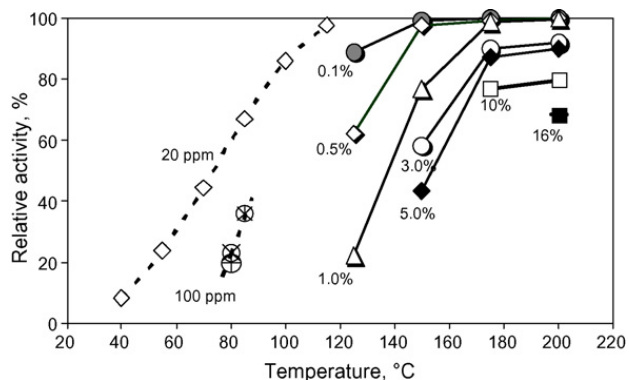
Fig. 9. The relative activity of the platinum catalyst for hydrogen oxidation as a function of temperature at different CO concentrations [37]. Dotted curves were for Nafion-based cells. Data for 20 ppm CO at 40–115 °C and for 100 ppm CO at 85 °C were from [245]. Data for 100 ppm CO at 80 °C were taken from [246,247] [reproduced from Li et al. with permission of The Electrochemical Society].

97% was observed for 20 ppm CO above 115 °C, for 0.5% CO above 150 °C, and for 1% CO above 175 °C.

Limited information on the H_2S poisoning effect is available. For PAFC at 190–205 °C, it was suggested that the total amount of sulphur containing compounds (H_2S and COS) in the fuel stream should not exceed 50 ppm with a maximum H_2S level of 20 ppm provided that the CO partial pressure does not exceed 2% [248]. For low temperature PEMFC, H_2S contents of below 1 ppm were suggested [249,250]. Recently Shi et al. have shown the electrochemical dependence of the H_2S poisoning effect [251] and demonstrated the recovery of the 1 kW stack performance by a potential cycling [252].

For PBI-based HT-PEMFC, Schmidt and Baurmeister [248] have demonstrated that, in the range of 10 ppm H_2S and 1% CO, the poisoning effects of these two impurities are additive, though the poisoning effect of H_2S may not be completely reversible (see Fig. 10). At 180 °C, a PBI-cell has been operating on reformate containing 5 ppm H_2S and 2% CO for more than 3000 h with a degradation rate of 20 μV h^{-1}, similar to that for operation with pure hydrogen, indicating the good tolerance ability. It should be remarked
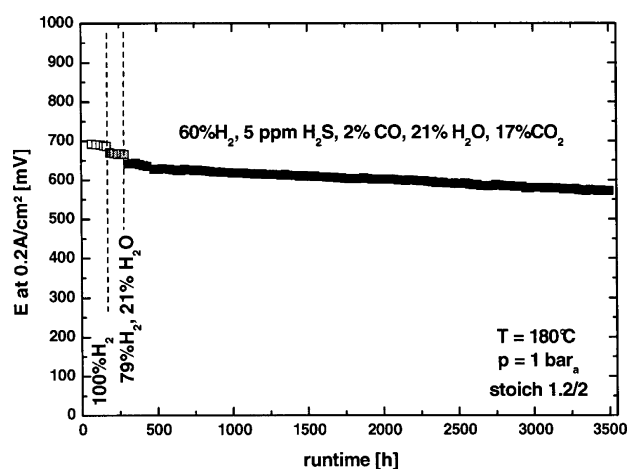

Fig. 10. Durability of a Celtec®-P1000 MEA at 180 °C and 1 bar absolute using realistic reformate as denoted in the figure [248] [reproduced from Schmidt and Bauemeister with permission of the Electrochemical Society].
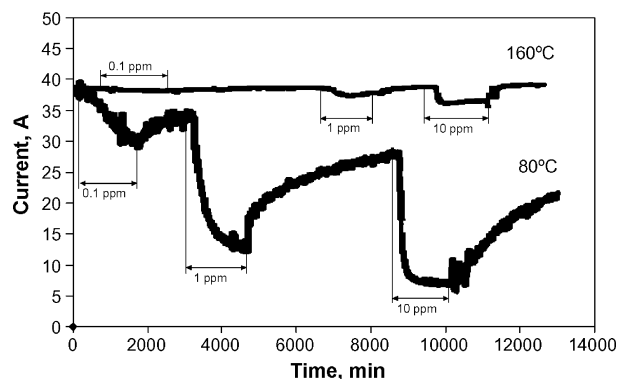

Fig. 11. SO_2 tolerance at cathode side of HT PEM fuel cell at 160 °C, compared to LT PEM fuel cell at 80 °C [253] [reproduced from Hubner, Huslage and Seyfried with permission of the Volkswagen fuel cell research group].

that this 10 ppm H_2S is a higher level than the current fuel processor and shift catalysts can tolerate over time.

Contamination of the cathode air is often underestimated and little information is available for PEMFC though the presence of traces of, e.g. sulphur dioxide is well known both in urban and rural surroundings. Recently the Volkwagen group [253] has examined the effect. As can be seen from Fig. 11, a low temperature PEMFC operating at 80 °C partly irreversibly decreases performance to some extent already at 0.1 ppm SO_2 and significantly at above 1 ppm SO_2. A considerable advantage is observed for high temperature PEMFC, which showed little performance loss for the SO_2 content of 1 ppm and a small restorable performance loss at 10 ppm SO_2.

5.4. Direct use of methanol reformate and integration with fuel processors

A methanol reformer is often operated at temperatures of 250–330 °C, however, the methanol reforming is also possible at lower temperatures (180–230 °C [41]), though at a low rate of hydrogen production. The CO content in the reformate streams is in the tolerance range of the high temperature PEMFC, allowing the PEMFC to operate with reformed hydrogen directly from a reformer without further CO removal [41,254].

For methanol reforming, it is estimated that a fuel cell stack produces about 3 times of the heat and water that a methanol steam reformer needs. This opens the possibility for an integration of the high temperature PEMFC with a methanol reformer. Holladay et al. [40] and Pan et al. [41] demonstrated the feasibility of an integrated methanol reformer and a PBI cell. This integration would have the advantages of higher efficiency and simple construction and operation. A reformed methanol fuel cell system was developed recently, as a chemically and thermally robust power source in the 2–10 W range [255]. Ultracell has constructed miniature methanol reformer/fuel cell systems as a battery recharger with a power range of 5–100 W [51]. Some calculations of energy savings through integration of a high temperature PEMFC with a methane or methanol reformer can be found in [39].

Another possibility is integration of PBI cells with a high capacity metal hydride hydrogen tank [38]. Sodium alanate,

for example, can store 4–5 wt% hydrogen reversibly with a desorption temperature of around 150 °C [256]. As hydrogen release from a hydride is a highly endothermic process heat is needed at the desorption temperature. In this case there is a much better match with the HT-PEMFC than with a conventional PEMFC. A simple system of a 6 cell PBI stack thermally integrated with an alanate tank was made at Sandia National Laboratory [257].

5.5. Durability issues

One of the most significant challenge for PBI membranes and their fuel cells is to improve lifetime. 40,000 h of operation for stationary uses and 5000 h of operation for automobile uses are commonly required with limited performance decay, say, less than 10%.

The reasons for failure of a PEMFC are numerous and not fully understood [258]. For PBI cells, the most likely mechanisms include (1) degradation of the polymer membranes due to the attack by, for example, H_2O_2 and its radicals (•OH or •OOH); (2) leaching of the doping acid from the membrane electrolyte; (3) loss of catalyst activities due to the catalyst sintering, catalyst dissolution and the carbon support corrosion.

5.5.1. Steady-state operation and acid loss

Fig. 12 shows a set of durability test results of PBI cells operating with hydrogen and oxygen under continuous operation at ambient pressure [223]. At temperatures around 150 °C a lifetime of 5000 h by continuous H_2/O_2 operation has been achieved at a constant cell voltage of 0.5 V. At temperatures above 180 °C, the lifetime is limited, and polymer oxidative degradation is likely the reason of the failure. As the attack by H_2O_2 and –OH and/or –OOH radicals is believed to be the principal degradation mechanism of polymer membranes, the Fenton test (see Fig. 4) showed significant degradation of PBI membranes, although they can be improved by crosslinking.

The oxidation by air seems much less than by pure oxygen. Using air, PEMEAS (now BASF) has demonstrated a lifetime of over 20,000 h at 160 °C [248]. From the result, a degradation rate of the cell performance is estimated to be about 5–6 $\mu V\,h^{-1}$. This performance degradation rate
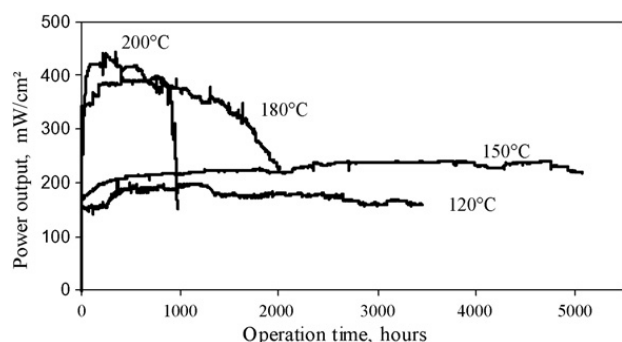

Fig. 12. Lifetime test of a PBI cell under continuous operation at different temperatures with hydrogen and oxygen at ambient pressure [223]. The membrane was fabricated from linear polymer with an average molecular weight of about 25,000 g mol⁻¹.

seems confirmed by Sartorius and Fumatech [94] as well as by Schmidt and Baurmeister [259].

Acid loss may occur through different mechanisms such as diffusion, capillary transport, membrane compression, evaporation, and especially, leaching by condensed water during shutdown and cold start. From the possible acid loss mechanisms, Staudt [238] estimated that, at a rate of 0.6 $\mu g\,m^{-2}\,s^{-1}$ at 160 °C, a full size 5 kW stack containing 2100 g of acid will be sufficient for 40,000 h of operation.

With acid-doped AB-PBI, however, Wannek et al. [260] reported a high degradation rate of 20–25 $\mu V\,h^{-1}$ under constant load. By collecting the acid from the offgas through a water condenser, they observed a constant acid loss (ca. 0.2 $\mu g\,m^{-2}\,s^{-1}$) at the cathode but only initially an acid loss (also ca. 0.2 $\mu g\,m^{-2}\,s^{-1}$) at the anode [240,260]. This was confirmed by the nearly constant resistance through the test period of 1000 h, indicating that the acid loss does not seem to be the main reason for the performance degradation.

Similar measurements were made by Yu et al. [98] under both steady-state and dynamic (load, thermal and shutdown-startup cycling) conditions. For steady-state operation a voltage degradation rate of 4.9–6.3 $\mu V\,h^{-1}$ was reported at 160 °C. In the temperature range of 80–160 °C the phosphoric acid loss rate was less than 10 $ng\,cm^{-2}\,h^{-1}$ or 0.03 $\mu g\,m^{-2}\,s^{-1}$, corresponding to a total acid of 2.6% after 40,000 h of steady-state operation.

5.5.2. Dynamic test

Continuous operation at temperatures above 100 °C involves no formation of liquid water and therefore less risk of acid leaching. During dynamic tests with thermal, load and shutdown–startup cycling, the amount and the vapour pressure of the water product varies and formation of liquid water might be involved. In addition, the shutdown–startup or/and temperature cycling cause thermal and mechanical stresses to the membranes and cell components as well as the volume expansion and contractions of the acid in MEAs. Another important mechanism of the cell degradation involved in these dynamic tests is the corrosion of carbon support and sintering of noble metal catalysts, as to be discussed in Section 5.5.3.

A thermal cycling test on a hydrogen-air cell with a daily shutdown and restart was performed by one of the authors' group. As shown in Fig. 13, over the first 60 daily cycles, a performance loss rate of 0.7 $mW\,cm^{-2}$ per cycle was observed. This performance loss is significant compared with that for the steady-state operation. In the following period of test over a period of more than 3 years, up to 850 cycles have been carried out showing a more or less stabilized performance, however, with a sudden death at the end. The sudden death was apparently due to the breakdown of the polymer membrane, as an abnormal increase in the gas permeability occurred. A performance loss rate of 0.07 $mW\,cm^{-2}$ per cycle, corresponding approximately to a voltage drop rate of 0.3 mV per cycle or 40 μV per operating hour was observed over the whole test period.

Based on the commercial Celtec®-P1000 MEA, Calundann [261] and Schmidt and Baurmeister [259] reported a similar daily startup–shutdown cycling test (12 h of operation at 160 °C followed by 12 h of shutdown). After a
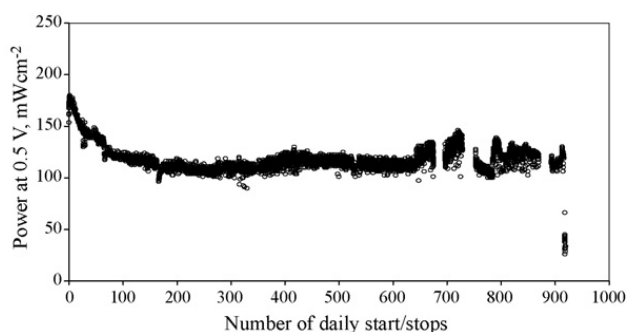
Fig. 13. A daily startup–shutdown cycling test of a PBI cell operating with hydrogen and air at 150 °C and ambient pressure. The calendar time was more than 3 years. The membrane was doped with 5.6 mol H_3PO_4. Catalyst loading for both electrodes was 0.61 mg Pt cm^{-2}. The cell was turned on ca. 7 h every working day through the period of time.

period of 6500 h with 260 cycles under mild conditions (160 °C and H_2), an average voltage drop of 0.3 mV per cycle was observed, corresponding to a performance loss of ca. 11 μV h^{-1} [259,261]. With the newly developed Celtec®-P2000 MEA, improved cycling performance of 15 μV h^{-1} under harsh conditions (180 °C and reformate) has been reported.

Based on the advanced PBI MEAs, the Volkswagen group performed a temperature cycle test between 160 and 40 °C. The cell operated for 2 h at 160 °C and 0.6 V and for 2 h at 40 °C and 0.6 V, as shown partly in Fig. 14. These test conditions are critical for acid-doped membranes because of the formation of liquid water, but prerequisite for automobile applications. With a specially designed complex membrane and electrode interfacial structure, a cycling test has been managed for operation of up to 2500 h, with a degradation rate of 6% power loss for every 1000 h [253]. For comparison purpose, a degradation rate could be estimated to be about 44 μV h^{-1}, if assuming the test was performed at a constant current density (830 mA cm^{-2}).

Staudt [238] reported another load test, by using the so called "filled" PBI membranes, with an off time (open circuit voltage) of 2 min and an on time at 0.2 A cm^{-2} of 30 min and at 0.6 A cm^{-2} for 30 min. Little performance degradation was observed in the first 600 h. The performance loss was estimated to be about 20 μV h^{-1} at OCV, 12 μV h^{-1} at
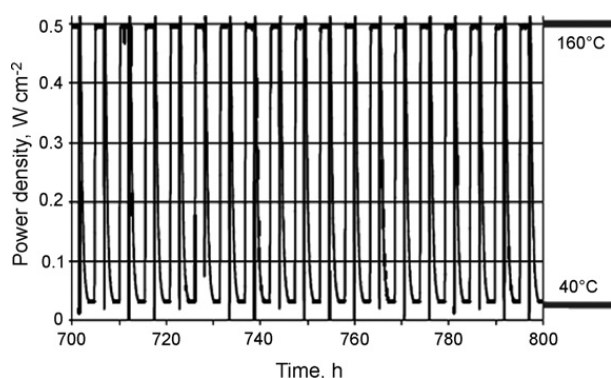

Fig. 14. Temperature cycling test between 160 and 40 °C. The periodic temperature cycle was 2 h at 160 °C and 2 h at 40 °C [253] [reproduced from Hubner, Huslage and Seyfried with permission of the Volkswagen fuel cell research group].

0.2 A cm^{-2} and 19 μV h^{-1} at 0.6 A cm^{-2}, respectively, based on which a lifetime of 14,000 h was projected.

5.5.3. Catalyst degradation

For low temperature PEMFC, corrosion of the carbon support and sintering of noble metal catalysts have been recognized as the main reason of PEMFC performance degradation [262,263]. This will be obviously aggravated at elevated temperatures.

Based on Vulcan carbon as the catalyst support, Zhai et al. [229] observed that, after a constant current (640 mA cm^{-2}) operation for over 500 h, the mean particle size of Pt increased from 4.02 to 8.88 nm, indicating that this might be a main reason of the early performance loss of PBI cells [230]. Under an OCV operation at 180 °C for 224 h, Qi and Buelte [264] found that the cathodic platinum particle size increases by 5 times, whereas the anodic catalyst particle size remains unchanged. It seems that the carbon corrosion is of more electrochemical nature, depending on the electrode potential.

Heat-treatments of carbon blacks at elevated temperatures is known to be able to impart graphite character to the carbon black and therefore increase its resistance to corrosion [265,266], however, at expense of a dramatic loss of the specific surface area. Recent studies showed that the specific surface area loss was primarily due to the elimination of pores less than 2.5 nm, which may not be available for the catalyst loading [267].

Liu et al. [268] introduced ZrO_2 into the carbon support in preparing 40% Pt catalysts for PBI cells. After 3000 cycles between 0.6 and 1.2 V, the ZrO_2/C-supported catalyst showed a decay rate of 6 and 12 μV/cycle at a current density of 100 and 1000 mA cm^{-2}, respectively, compared to 9 and 28 μV/cycle for the Pt/C based cathode. An accelerated ageing test was performed by immersing the catalysts in concentrated phosphoric acid saturated with air at 204 °C for 5 h, which is believed to simulate 2000 h of PAFC operation. ZrO_2/C supported Pt catalysts showed higher sintering resistance and corrosion resistance [269]. The highly dispersed Pt atoms seem to be obstructed by the adjacent ZrO_2 and the agglomeration of Pt particles could be inhibited.

To summarize the discussion of this section, it seems that a degradation rate of only 5 μV h^{-1} can be expected under continuous operation with hydrogen and air at 150–160 °C. By defining a failure as 10% performance loss from 0.6 V, this degradation rate corresponds to a lifetime of 12,000 h. For stationary uses aiming at 40,000 h, this lifetime needs to be further improved. Upon thermal or/and load on/off cyclings, which are more relevant to automobile applications, a performance loss of 300 μV per cycle or 40 μV per operating hours has been reported, attributable to more serious acid leaching due to the liquid water formation and the cathodic catalyst activity loss because of exposure to OCV.

6. Conclusive remarks

The phosphoric acid-doped polybenzimidazole membrane seems so far the most successful system for high

temperature PEMFC preferably under ambient pressure. It has in recent years motivated extensive research activities covering polymer synthesis, membrane casting, physico-chemical characterizations and fuel cell technologies. To optimize the membrane properties, high molecular weight polymers with synthetically modified or N-substituted structures have been synthesized. Techniques for membrane casting from organic solutions and directly from TFA and PPA solutions have been explored. Ionic and covalent cross-linking as well as inorganic–organic composites has been developed. Acid-doped PBI membranes have been extensively characterized.

Related fuel cell technologies have been developed and high temperature PEMFC has been successfully demonstrated at temperatures of up to 200 °C under ambient pressure. No gas humidification is mandatory, which enables the elimination of the complicated humidification system, compared with Nafion cells. Other operating features of the PBI cell include easy control of air flow rate and cell temperature (in a wider range). The latter, together with the increased temperature gradient, will potentially simplify the cooling system. The PBI cell operating at above 150 °C can tolerate up to 1% CO and 10 ppm SO_2 in the fuel stream, allowing for simplification of the fuel processing system and possible integration of the fuel cell stack with fuel processing units.

Long-term durability with a degradation rate of $5-10 \mu V h^{-1}$ has been achieved under continuous operation with hydrogen and air at 150–160 °C. With load or thermal cycling, a performance loss of $300 \mu V$ per cycle or $40 \mu V h^{-1}$ per operating hour has been observed. Further improvement should be done by, e.g. optimizing the thermal and chemical stability of the polymer, acid–base interaction and acid management, activity and stability of catalyst and more importantly the catalyst support, as well as the integral interface between electrode and membrane.

Other issues than durability that have to be addressed in further development include (1) the low proton conductivity, especially in the low temperature range, which is of importance for the cold start; (2) slow oxygen reduction kinetics due to the strong surface adsorption of acid anions and low solubility (and diffusivity) of oxygen; (3) fundamental materials and techniques of stack construction, including selection and evaluation of bipolar plates, seals (integrated sealing is very much desired to strengthen the membrane and improve the acid management) and coolant/cooling; and (4) system simulation and design with respect to thermal management, heat recovery, water balance as well as the possible integration of stack with fuel processing units.

Acknowledgements

References

[1] Costamagna P, Srinivasan S. Quantum jumps in the PEMFC science and technology from the 1960s to the year 2000. J Power Sources 2001;102:242–52, 253–69.

[2] Li QF, He RH, Jensen JO, Bjerrum NJ. Approaches and recent development of polymer electrolyte membranes for fuel cells operating above 100 °C. Chem Mater 2003;15:4896–915.

[3] Yang C, Costamagna P, Srinivasan S, Benziger J, Bocarsly AB. Approaches and technical challenges to high temperature operation of proton exchange membrane fuel cells. J Power Sources 2001;103:1–9.

[4] Zhang JL, Xie Z, Zhang JJ, Tanga YH, Song CJ, Navessin T, et al. High temperature PEM fuel cells. J Power Sources 2006;160:872–91.

[5] Shao YY, Yin GP, Wang ZB, Gao YZ. Proton exchange membrane fuel cell from low temperature to high temperature: material challenges. J Power Sources 2007;167:235–42.

[6] Jones DJ, Roziére J. Recent advances in the functionalisation of polybenzimidazole and polyetherketone for fuel cell applications. J Membr Sci 2001;185:41–58.

[7] Rikukawa M, Sanui K. Proton-conducting polymer electrolyte membranes based on hydrocarbon polymers. Prog Polym Sci 2000;25:1463–502.

[8] Harrison WL, Hickner MA, Kim YS, McGrath JE. Poly(arylene ether sulphone) copolymers and related systems from disulphonated monomer building blocks: synthesis, characterization, and performance—a topical review. Fuel Cells 2005;5:201–12.

[9] Jagur-Grodzinski J. Polymeric materials for fuel cells: concise review of recent studies. Polym Adv Technol 2007;18:785–99.

[10] Jones DJ, Roziére J. Inorganic/organic composite membranes. In: Vielstichm W, Lamm A, Gasteiger HA, editors. Handbook of fuel cells, vol. 3. John Wiley & Sons Ltd.; 2003. p. 447–63.

[11] Ogoshi T, Chujo Y. Organic–inorganic polymer hybrids prepared by the sol–gel method. Compos Interf 2005;11:539–66.

[12] Herring AM. Inorganic–polymer composite membranes for proton exchange membrane fuel cells. J Macromol Sci C: Polym Rev 2006;46:245–96.

[13] Wainright JS, Litt MH, Savinell RF. High temperature membranes. In: Vielstichm W, Lamm A, Gasteiger HA, editors. Handbook of fuel cells, vol. 3. John Wiley & Sons Ltd.; 2003. p. 436–46.

[14] Li QF, He RH, Jensen JO, Bjerrum NJ. PBI-based polymer membranes for high temperature fuel cells—preparation, characterization and fuel cell demonstration. Fuel Cells 2004;4:147–59.

[15] Asensio JA, Gomez-Romero P. Recent developments on proton conducting poly(2,5-benzimidazole) (AB-PBI) membranes for high temperature polymer electrolyte membrane fuel cells. Fuel Cells 2005;5:336–43.

[16] Kerres JA. Blended and cross-linked ionomer membranes for application in membrane fuel cells. Fuel Cells 2005;5:230–47.

[17] Lasségues JC. Mixed Inorganic–organic systems: the acid/polymer blends. In: Colomban Ph, editor. Proton conductors, solids, membranes and gels—materials and devices. Cambridge Univ. Press; 1992. p. 311–28.

[18] Schuster M, Rager T, Noda A, Kreuer KD, Maier J. About the choice of the protogenic group in PEM separator materials for intermediate temperature, low humidity operation: a critical comparison of sulphonic acid, phosphonic acid and imidazole functionalized model compounds. Fuel Cells 2005;5:355–65.

[19] Paddison SJ, Kreuer KD, Maier J. About the choice of the protogenic group in polymer electrolyte membranes: ab initio modelling of sulphonic acid, phosphonic acid, and imidazole functionalized alkanes. Phy Chem Chem Phys 2006;8:4530–42.

[20] Steininger H, Schuster M, Kreuer KD, Kaltbeitzel A, Bingol B, Meyer WH, et al. Intermediate temperature proton conductors for PEM fuel cells based on phosphonic acid as protogenic group: a progress report. Phy Chem Chem Phys 2007;9:1764–73.

[21] Wainright JS, Wang JT, Weng D, Savinell RF, Litt M. Acid-doped polybenzimidazoles—a new polymer electrolyte. J Electrochem Soc 1995;142:L121–3.

[22] Savinell RF, Litt MH. Proton conducting polymers used as membranes (Case Western Reserve University). US patent 5,525,436 (1996).

[23] (a) Savinell RF, Litt MH. Proton conducting polymers prepared by direct acid casting (Case Western Reserve University). US patent 5,716,727 (1998).;
(b) Savinell RF, Litt MH. Proton conducting solid polymer electrolytes prepared by direct acid casting (Case Western Reserve University). US patent 6,025,085 (2000).;
(c) Savinell RF, Litt MH. Proton conducting polymers prepared by direct acid casting (Case Western Reserve University). US patent 6,099,988 (2000).

[24] (a) Sansone MJ, Onorato FJ, Ogata N. Acid-modified polybenzimidazole fuel cell elements (Hoechst Celanese Corporation). US patent 5,599,639 (1997).;
(b) Yamamoto T. Method for producing bridged polymer membrane and fuel cell (Celanese Ventures GmbH). US patent 6,790,553 (2004).;
(c) Onorato FJ, Sansone MJ, French SM, Marikar F. Process for producing polybenzimidazole pastes and gels for use in fuel cells (Aventis Research & Technologies GmbH & Co. KG). US patent 5,945,233 (1999).;
(d) Onorato FJ, Sansone MJ, Kim DW, French SM, Marikar F. Process for producing polybenzimidazole fabrics for use in fuel cells (Aventis Research & Technologies GmbH & Co. KG). US patent 6,042,968 (2000).;
(e) Sansone MJ, Onorato FJ, French SM, Marikar F. Process for producing polymeric films for use as fuel cells (Celanese Ventures GmbH). US patent 6,187,231 (2001).

[25] (a) Akita H, Ichikawa M, Nosaki K, Oyanagi H, Iguchi M. Solid polymer electrolytes (Honda). US patent 6,124,060 (2000).;
(b) Oyanagi H, Sato S, Ise M, Okamoto T. Method of operating phosphoric acid fuel cell (Honda). US patent 6,833,204 (2004).;
(c) Okamoto T, Okazaki K, Sato S. Fuel cell system (Honda). US patent 6,815,109 (2004).

[26] (a) Li C, Lian KK, Eschbach FO. Electrochemical cell having a polymer electrolyte (Motorola, Inc.). US patent 5,688,613 (1997).;
(b) Wu H, Li C, Lian KK. Polymer electrolyte and an electrochemical cell containing the electrolyte (Motorola, Inc.). US patent 5,723,231 (1998).

[27] Bjerrum NJ, Li Q, Hjuler HA. Polymer electrolyte membrane fuel cells (Danish Power Systems). US patent 6,946,211 and EP 1,523,053 (2002).

[28] (a) Huang WW. Integrated fuel cell system (Plug Power Inc.). US patent 6,753,107 (2004).;
(b) Ingraham JE, Cutright, Richard H. Integrated fuel cell system (Plug Power Inc.). US patent 6,913,846 (2005).

[29] Bouchet R, Siebert E. Proton conduction in acid doped polybenzimidazole. Solid State Ionics 1999;118:287–99.

[30] Glipa X, Bonnet B, Mula B, Jones DJ, Roziere J. Investigation of the conduction properties of phosphoric and sulfuric acid doped polybenzimidazole. J Mater Chem 1999;9:3045–9.

[31] Kawahara M, Morita J, Rikukawa M, Sanui K, Ogata N. Synthesis and proton conductivity of thermally stable polymer electrolyte: poly(benzimidazole) complexes with strong acid molecules. Electrochim Acta 2000;45:1395–8.

[32] He RH, Li QF, Xiao G, Bjerrum NJ. Proton conductivity of phosphoric acid doped polybenzimidazole and its composites with inorganic proton conductors. J Membr Sci 2003;226:169–84.

[33] Ma YL, Wainright JS, Litt MH, Savinell RF. Conductivity of PBI membranes for high-temperature polymer electrolyte fuel cells. J Electrochem Soc 2004;151:A8–16.

[34] Litt M, Ameri R, Wang Y, Savinell R, Wainwright J. Polybenzimidazoles/phosphoric acid solid polymer electrolytes: mechanical and electrical properties. Mater Res Soc Symp Proc 1999;548:313–23.

[35] Samms SR, Wasmus S, Savinell RF. Thermal stability of proton conducting acid doped polybenzimidazole in simulated fuel cell environments. J Electrochem Soc 1996;143:1225–32.

[36] Wang JT, Savinell RF, Wainright JS, Litt M, Yu H. A H_2/O_2 fuel cell using acid doped polybenzimidazole as polymer electrolyte. Electrochim Acta 1996;41:193–7.

[37] Li QF, He RH, Gao JA, Jensen JO, Bjerrum NJ. The CO poisoning effect in PEMFCs operational at temperatures up to 200 °C. J Electrochem Soc 2003;150:A1599–605.

[38] Jensen JO, Li Q, He R, Pan C, Bjerrum NJ. 100–200 °C polymer fuel cells for use with NaAlH$_4$. J Alloys Compd 2005;404–406:653–6.

[39] Jensen JO, Li QF, Pan C, Vestbo AP, Mortensen K, Petersen HN, et al. High temperature PEMFC and the possible utilization of the excess heat for fuel processing. Int J Hydrogen Energy 2007;32:1567–71.

[40] Holladay JD, Wainright JS, Jones EO, Gano SR. Power generation using a mesoscale fuel cell integrated with a microscale fuel processor. J Power Sources 2004;130:111–8.

[41] Pan C, He RH, Li QF, Jensen JO, Bjerrum NJ, Hjulmand HA, et al. Integration of high temperature PEM fuel cells with a methanol reformer. J Power Sources 2005;149:392–8.

[42] Cheddie D, Munroe N. Analytical correlations for intermediate temperature PEM fuel cells. J Power Sources 2006;160:299–304.

[43] Cheddie D, Munroe N. Parametric model of an intermediate temperature PEMFC. J Power Sources 2006;156:414–23.

[44] Cheddie D, Munroe N. Mathematical model of a PEMFC using a PBI membrane. Energy Convers Manage 2006;47:1490–504.

[45] Peng J, Lee SJ. Numerical simulation of proton exchange membrane fuel cells at high operating temperature. J Power Sources 2006;162:1182–91.

[46] Scott K, Pilditch S, Mamlouk M. Modelling and experimental validation of a high temperature polymer electrolyte fuel cell. J Appl Electrochem 2007;37:1245–59.

[47] Zenith F, Seland F, Kongstein OE, Borresen B, Tunold R, Skogestad S. Control-oriented modelling and experimental study of the transient response of a high-temperature polymer fuel cell. J Power Sources 2006;162:215–27.

[48] Korsgaard AR, Refshauge R, Nielsen MP, Bang M, Kaer SK. Experimental characterization and modeling of commercial polybenzimidazole-based MEA performance. J Power Sources 2006;162:239–45.

[49] Korsgaard AR, Nielsen MP, Kaer SK. A novel model of HTPEM-based micro-combined heat and power fuel cell system. Int J Hydrogen Energy 2008;33:1909–20.

[50] Korsgaard AR, Nielsen MP, Kaer SK. Control of a novel model of HTPEM based micro combined heat and power fuel cell system. Int J Hydrogen Energy 2008;33:1921–31.

[51] Membranes and electrodes for fuel cells as PEMEAs merges with E-TEK. Fuel cell bulletin 2006, no. 2. p. 12–5.

[52] Perry KA, Eisman GA, Benicewicz BC. Electrochemical hydrogen pumping using a high-temperature polybenzimidazole (PBI) membrane. J Power Sources 2008;177:478–84.

[53] Bouchet R, Siebert E, Vitter G. Polybenzimidazole-based hydrogen sensors I. Mechanism of response with an E-TEK gas diffusion electrode. J Electrochem Soc 2000;147:3125–30.

[54] Bouchet R, Siebert E, Vitter G. Polybenzimidazole-based hydrogen sensors—II. Effect of the electrode preparation. J Electrochem Soc 2000;147:3548–51.

[55] Rosini S, Siebert E. Solid-state internal reference electrode based on quinhydrone for hydrogen sensor with acid-doped polybenzimidazole. Electrochim Acta 2004;49:525–36.

[56] Neuse EW. Aromatic polybenzimidazoles—syntheses, properties and applications. Adv Polym Sci 1982;47:1–42.

[57] Cassidy PE. Thermally stable polymers. New York: Marcel Dekker, Inc.; 1980.

[58] Chung TS. A critical review of polybenzimidazoles: historical development and future R&D. J Macromol Sci 1997;C37:277–301.

[59] Marikar YMF, Besso MM. Electrically conductive polybenzimidazole fibrous material (Hoechst Celanese Corporation). US patent 4,759,986 (1988).

[60] Marikar YMF, Besso MM. Process for preparing electrically conductive shaped articles from polybenzimidazoles (Hoechst Celanese Corporation). US patent 5,017,420 (1991).

[61] Brinegar WC. Reverse osmosis process employing polybenzimidazole membranes (Celanese Corporation). US patent 3,720,607 (1973).

[62] Boom AA. Production of improved semipermeable polybenzimidazole membranes (Celanese Corporation). US patent 3,737,042 (1973).

[63] Brinegar WC. Production of semipermeable polybenzimidazole membranes (Celanese Corporation). US patent 3,841,492 (1974).

[64] Wang DGJ. Process for the production of semipermeable polybenzimidazole membranes with low temperature annealing (Celanese Corporation). US patent 4,448,687 (1984).

[65] Wang DGJ. Process for the production of semipermeable polybenzimidazole membranes and the resultant product (Celanese Corporation). US patent 4,512,894 (1985).

[66] Sansone MJ. Process for the production of polybenzimidazole ultrafiltration membranes (Celanese Corporation). US patent 4,693,824 (1987).

[67] Trouw NS. Method for the preparation of polybenzimidazole membranes (Celanese Corporation). US patent 4,693,825 (1987).

[68] Chung TS, Xu ZL. Asymmetric hollow fiber membranes prepared from miscible polybenzimidazole and polyetherimide blends. J Membr Sci 1998;147:35–47.

[69] Pesiri DR, Jorgensen B, Dye RC. Thermal optimization of poly-benzimidazole meniscus membranes for the separation of hydrogen, methane, and carbon dioxide. J Membr Sci 2003;218:11–8.

[70] Kumbharkar SC, Karadkar PB, Kharul UK. Enhancement of gas permeation properties of polybenzimidazoles by systematic structure architecture. J Membr Sci 2006;286:161–9.

[71] Chanda M, Rempel GL. Polybenzimidazole resin-based new chelating-agents—uranyl and ferric ion selectivity of resins with anchored dimethylglyoxime. React Polym 1989;11:165–76.

[72] Chanda M, Rempel GL. Polybenzimidazole resin based new chelating-agents—palladium(II) and platinum(IV) sorption on resin with immobilized dithiooxamide. React Polym 1990;12:83–94.

[73] Chanda M, Rempel GL. Polybenzimidazole resin based new chelating-agents—uranyl-ion selectivity of resins with immobilized glyoxal-bis-2-hydroxyanil and salicylaldehyde-ethylenediimine. React Polym 1990;13:103–19.

[74] Chanda M, Rempel GL. Removal of uranium from acidic sulfate-solution by ion-exchange on poly(4-vinylpyridine) and polybenzimidazole in protonated sulfate form. React Polym 1992;17:159–74.

[75] Chanda M, Rempel GL. Separation of hydroxycitric acid lactone from fruit pectins and polyhydroxyphenols on polybenzimidazole weak-base resin. Ind Eng Chem Res 1999;38:2474–81.

[76] Vogel H, Marvel CS. Polybenzimidazoles, new thermally stable polymers. J Polym Sci 1961;50:511–39.

[77] Choe EW. Catalysts for the preparation of polybenzimidazoles. J Appl Polym Sci 1994;53:497–506.

[78] Choe EW. Single-stage melt polymerization process for the production of high molecular weight polybenzimidazole (Celanese Corporation). US patent 4,312,976 (1982).

[79] Choe EW, Choe DD. Polybenzimidazoles (overview). In: Salamone JC, editor. Polymeric materials encyclopedia, vol. 7. New York: CRC Press; 1996. p. 5619–38.

[80] Iwakura Y, Imai Y, Uno K. Polyphenylenebenzimidazoles. J Polym Sci 1964;2A:2605–15.

[81] Lobato J, Canizares P, Rodrigo MA, Linares JJ, Manjavacas G. Synthesis and characterisation of poly[2,2-(m-phenylene)-5,5-bibenzimidazole] as polymer electrolyte membrane for high temperature PEMFCs. J Membr Sci 2006;280:351–62.

[82] Hedberg FL, Marvel CS. New single-step process for polybenzimidazole synthesis. J Polym Sci 1974;12:1823–8.

[83] Eaton PE, Carlson GR, Lee JT. Phosphorus pentoxide-methanesulphonic acid—convenient alternative to polyphosphoric acid. J Org Chem 1973;38:4071–3.

[84] Kim HJ, Cho SY, An SJ, Kim JY, Eun YC, Kim JY, et al. Synthesis of poly(2,5-benzimidazole) for use as a fuel-cell membrane. Macromol Rapid Commun 2004;25:894–7.

[85] Jouanneau J, Mercier R, Gonon L, Gebel G. Synthesis of sulphonated polybenzimidazoles from functionalized monomers: preparation of ionic conducting membranes. Macromolecules 2007;40:983–90.

[86] Sannigrahi A, Arunbabu D, Sankar RM, Jana T. Tuning the molecular properties of polybenzimidazole by copolymerisation. J Phys Chem B 2007;111:12124–32.

[87] Kim TH, Lim TW, Lee JC. High-temperature fuel cell membranes based on mechanically stable para-ordered polybenzimidazole prepared by direct casting. J Power Sources 2007;172:172–9.

[88] Xiao LX, Zhang HF, Scanlon E, Ramanathan LS, Choe EW, Rogers D, et al. High-temperature polybenzimidazole fuel cell membranes via a sol–gel process. Chem Mater 2005;17:5328–33.

[89] Xiao L, Zhang H, Jana T, Scanlon E, Chen R, Choe EW, et al. Synthesis and characterization of pyridine-based polybenzimidazoles for high temperature polymer electrolyte membrane fuel cell applications. Fuel Cells 2005;5:287–95.

[90] Kovar RF, Arnold FE. Para-ordered polybenzimidazole. J Polym Sci Polym Chem 1976;14:2807–17.

[91] Kallitsis JK, Gourdoupi N. Proton conducting membranes based on polymer blends for use in high temperature PEM fuel cells. J New Mater Electrochem Sys 2003;6:217–22.

[92] Daletou MK, Gourdoupi N, Kallitsis JK. Proton conducting membranes based on blends of PBI with aromatic polyethers containing pyridine units. J Membr Sci 2005;252:115–22.

[93] Carollo A, Quartarone E, Tomasi C, Mustarelli P, Belotti F, Magistris A, et al. Developments of new proton conducting membranes based on different polybenzimidazole structures for fuel cells applications. J Power Sources 2006;160:175–80.

[94] See Li QF, Jensen OJ. Membranes for high temperature PEMFC based on acid-doped polybenzimidazoles. In: Peinemann KV, Nunes SP, editors. Membranes for energy conversion, vol. 6. Wiley-VCH; 2007. p. 61–96.

[95] Asensio JA, Borro S, Gomez-Romero P. Polymer electrolyte fuel cells based on phosphoric acid-impregnated poly(2,5-benzimidazole) membranes. J Electrochem Soc 2003;151:A304–10.

[96] Asensio JA, Borros S, Gomez-Romero P. Proton-conducting membranes based on poly(2,5-benzimidazole) (AB-PBI) and phosphoric acid prepared by direct acid casting. J Membr Sci 2004;241:89–93.

[97] Qing SB, Huang W, Yan DY. Synthesis and characterization of thermally stable sulphonated polybenzimidazoles. Eur Polym J 2005;41:1589–95.

[98] Yu S, Xiao L, Benicewicz BC. Durability studies of PBI-based high temperature PEMFCs. Fuel Cells 2008;8:156–74.

[99] Chuang SW, Hsu SLC. Synthesis and properties of a new fluorine-containing polybenzimidazole for high-temperature fuel-cell applications. J Polym Sci A 2006;44:4508–13.

[100] Chuang SW, Hsu SLC, Hsu CL. Synthesis and properties of fluorine-containing polybenzimidazole/montmorillonite nanocomposite membranes for direct methanol fuel cell applications. J Power Sources 2007;168:172–7.

[101] Qing SB, Huang W, Yan DY. Synthesis and properties of soluble sulphonated polybenzimidazoles. React Funct Polym 2006;66:219–27.

[102] Asensio JA, Borros S, Gomez-Romero P. Proton-conducting polymers based on benzimidazoles and sulphonated benzimidazoles. J Polym Sci A: Polym Chem 2002;40:3703–10.

[103] Qing SB, Huang W, Yan DY. Synthesis and characterization of thermally stable sulphonated polybenzimidazoles obtained from 3,3′-disulphonyl-4,4′-dicarboxyldiphenylsulphone. J Polym Sci A: Polym Chem 2005;43:4363–72.

[104] Xu HJ, Chen KC, Guo XX, Fang JH, Yin J. Synthesis of hyperbranched polybenzimidazoles and their membrane formation. J Membr Sci 2007;288:255–60.

[105] Xu HJ, Chen KC, Guo XX, Fang JH, Yin J. Synthesis and properties of hyperbranched polybenzimidazoles via A(2)+B-3 approach. J Polym Sci A: Polym Chem 2007;45:1150–8.

[106] Bower EA, Rafalko JJ. Process for modifying polybenzimidazole polymers with ethylene carbonates (Celanese Corporation). US patent 4,599,388 (1986).

[107] Sansone MJ, Gupta B, Stackman RW. Sulfoalkylation of polybenzimidazole (Hoechst Celanese). US patent 4,814,399 (1989).

[108] Sansone MJ, Gupta B, Forbes CE, Kwiatek MS. Sulfalkylation of hydroxyethylated polybenzimidazole polymers (Hoechst Celanese). US patent 4,997,892 (1991).

[109] Sansone MJ. Cyanoethylation of hydroxyethylated polybenzimidazole polymers (Hoechst Celanese). US patent 4,868,249 (1989).

[110] Sansone MJ, Kwiatek MS, Preparation of N-substituted phenyl polybenzimidazole polymers (Hoechst Celanese). US patent 4,933,397 (1990).

[111] Sansone MJ. N-substituted polybenzimidazole polymer (Hoechst Celanese). US patent 4,898,917 (1990).

[112] Klaehn JR, Luther TA, Orme CJ, Jones MG, Wertsching AK, Peterson ES. Soluble N-substituted organosilane polybenzimidazoles. Macromolecules 2007;40:7487–92.

[113] Pu HT, Liu GH. Preparation and proton conductivity of poly(N-methylbenzimidazole) doped with acid. Polym Adv Technol 2004;15:726–30.

[114] Pu HT, Liu QZ, Liu GH. Methanol permeation and proton conductivity of acid-doped poly (N-ethylbenzimidazole) and poly(N-methylbenzimidazole). J Membr Sci 2004;241:169–75.

[115] Pu HT, Liu GH. Synthesis and solubility of poly(N-methylbenzimidazole) and poly(N-ethylbenzimidazole): control of degree of alkylation. Polym Int 2005;54:175–9.

[116] Ariza MJ, Jones DJ, Roziere J. Role of post-sulphonation thermal treatment in conducting and thermal properties of sulfuric acid sulphonated poly(benzimidazole) membranes. Desalinatin 2002;147:183–9.

[117] Staiti P, Lufrano F, Arico AS, Passalacqua E, Antonucci V. Sulphonated polybenzimidazole membranes—preparation and physico-chemical characterization. J Membr Sci 2001;188:71–8.

[118] Gieselman MB, Reynolds JR. Water-soluble polybenzimidazole-based polyelectrolytes. Macromolecules 1992;25:4832–4.

[119] Gieselman MB, Reynolds JR. Aramid and imidazole based polyelectrolytes—physical-properties and ternary phase-behavior with poly(benzobisthiazole) in methanesulphonic-acid. Macromolecules 1993;26:5633–42.

[120] Spry RJ, Alexander MD, Bai SJ, Dang TD, Price GE, Dean DR, et al. Anisotropic ionic conductivity of lithium-doped sulphonated PBI. J Polym Sci 1997;35B:2925–33.

[121] Glipa X, Haddad ME, Jones DJ, Roziere J. Synthesis and characterisation of sulphonated polybenzimidazole: a highly conducting proton exchange polymer. Solid State Ionics 1997;97:323–31.

[122] Roziere J, Jones DJ, Marrony M, Glipa X, Mula B. On the doping of sulphonated polybenzimidazole with strong bases. Solid State Ionics 2001;145:61–8.

[123] Bae JM, Honma I, Murata M, Yamamoto T, Rikukawa M, Ogata N. Properties of selected sulphonated polymers as proton-conducting electrolytes for polymer electrolyte fuel cells. Solid State Ionics 2002;147:189–94.

[124] Kawahara M, Rikukawa M, Sanui K, Ogata N. Synthesis and proton conductivity of sulphopropylated poly(benzimidazole) films. Solid State Ionics 2000;136:1193–6.

[125] Kawahara M, Rikukawa M, Sanui K. Relationship between absorbed water and proton conductivity in sulphopropylated poly(benzimidazole). Polym Adv Technol 2000;11:544–7.

[126] Peron J, Ruiz E, Jones DJ, Roziere J. Solution sulfonation of a novel polybenzimidazole, a proton electrolyte for fuel cell application. J Membr Sci 2008;314:247–56.

[127] Xu HJ, Chen KC, Guo XX, Fang JH, Yin J. Synthesis of novel sulfonated polybenzimidazole and preparation of cross-linked membranes for fuel cell application. Polymer 2007;48:5556–64.

[128] Kim JH, Kim HJ, Lim TH, Lee HI. Dependence of the performance of a high-temperature polymer electrolyte fuel cell on phosphoric acid-doped polybenzimidazole ionomer content in cathode catalyst layer. J Power Sources 2007;170:275–80.

[129] Xing BZ, Savadogo O. The effect of acid doping on the conductivity of polybenzimidazole (PBI). J New Mater Electrochem Syst 1999;2:95–101.

[130] Pu HT, Meyer WH, Wegner G. Proton transport in polybenzimidazole blended with H_3PO_4 or H_2SO_4. J Polym Sci 2002;40B:663–9.

[131] Fontanella JJ, Wintersgill MC, Wainright JS, Savinell RF, Litt M. High pressure electrical conductivity studies of acid doped polybenzimidazole. Electrochim Acta 1998;43:1289–94.

[132] Ünsal Ö, Kiefer J. Polymer electrolyte membrane, method for the production thereof, and application thereof in fuel cells (Celanese Ventures GmbH). Patent WO03096465 (2003).

[133] Gubler L, Kramer D, Belack J, Ünsal Ö, Schmidt TJ, Scherer GG. Celtec.V—a polybenzimidazole-based membrane for the direct methanol fuel cell. J Electrochem Soc 2007;154:B981–7.

[134] Yamada M, Honma I. Anhydrous proton conducting polymer electrolytes based on poly(vinylphosphonic acid)-heterocycle composite material. Polymer 2005;46:2986–92.

[135] Erdemi H, Bozkurt A. Synthesis and characterization of poly (vinylpyrrolidone-co-vinylphosphonic acid) copolymers. Eur Polym J 2004;40:1925–9.

[136] Bingol B, Meyer WH, Wagner M, Wegner G. Synthesis, microstructure, and acidity of poly (vinylphosphonic acid). Macromol Rapid Commun 2006;27:1719–24.

[137] Lee YJ, Bingol B, Murakhtina T, Sebastiani D, Meyer WH, Wegner G, et al. High-resolution solid-state NMR studies of poly(vinyl phosphonic acid) proton-conducting polymer: molecular structure and proton dynamics. J Phys Chem B 2007;111:9711–21.

[138] Kerres J, Ullrich A, Meier F, Häring T. Synthesis and characterization of novel acid–base polymer blends for application in membrane fuel cells. Solid State Ionics 1999;125:243–9.

[139] Kerres J, Hein M, Zhang W. Development of new blend membranes for polymer electrolyte fuel cell applications. J New Mater Electrochem Syst 2003;6:223–30.

[140] Kerres J, Ullrich A, Häring Th, Baldauf M, Geghardt U, Preidel WJ. Preparation characterization and fuel cell application of new acid–base blend membranes. J New Mater Electrochem Syst 2000;3:229–39.

[141] Kerres J, Zhang W, Jorissen L, Gogel VJ. Application of different types of polyaryl-blend-membranes in DMFC. J New Mater Electrochem Syst 2002;5:97–107.

[142] Kerres J, Ullrich A, Hein M, Gogel V, Friedrich KA, Jorissen L. Cross-linked polyaryl blend membranes for polymer electrolyte fuel cells. Fuel Cells 2004;4:105–12.

[143] Jorissen L, Gogel V, Kerres J, Garche J. New membranes for direct methanol fuel cells. J Power Sources 2002;105:267–73.

[144] Guiver MD, Robertson GP. Chemical modification of polysulphones 2: an efficient method for introducing primary amine groups onto the aromatic chain. Macromolecules 1995;28:7612–21.

[145] Kerres J, Ullrich A, Hein M. Preparation and characterization of novel basic polysulphone polymers. J Polym Sci A: Polym Chem 2001;39:2874–88.

[146] Tang CM, Zhang W, Kerres J. Preparation and characterization of ionically cross-linked proton-conducting membranes. J New Mater Electrochem Syst 2004;7:287–98.

[147] Xing D, Kerres J. Improvement of synthesis procedure and characterization of sulphonated poly(arylene ether sulphone) for proton exchange membranes. J New Mater Electrochem Syst 2006;9:51–60.

[148] Xing D, Kerres J. Improved performance of sulphonated polyarylene ethers for proton exchange membrane fuel cells. Polym Adv Technol 2006;17:591–7.

[149] Kerres J, Ullrich A. Synthesis of novel engineering polymers containing basic side groups and their application in acid–base polymer blend membranes. Sep Purif Technol 2001;22–23:1–15.

[150] Kosmala B, Schauer J. Ion-exchange membranes prepared by blending sulphonated poly(2,6-dimethyl-1,4-phenylene oxide) with polybenzimidazole. Appl Polym Sci 2002;85:1118–27.

[151] Lee J, Kerres J. Synthesis and characterization of sulphonated poly(arylene thioether)s and their blends with polybenzimidazole for proton exchange membranes. J Membr Sci 2007;294:75–83.

[152] Wycisk R, Kee JK, Pintauro PN. Sulfonated polyphosphazene-polybenzimidazole membranes for DMFCs. J Electrochem Soc 2005;152:A892–8.

[153] Hobson LJ, Nakano Y, Ozu H, Hayase S. Targeting improved DMFC performance. J Power Sources 2002;104:79–84.

[154] Ainla A, Brandell D. Nafion-polybenzimidazole (PBI) composite membranes for DMFC applications. Solid State Ionics 2007; 178:581–5.

[155] Wycisk R, Chisholm J, Lee J, Lin J, Pintauro PN. Direct methanol fuel cell membranes from Nafion-polybenzimidazole blends. J Power Sources 2006;163:9–17.

[156] Zhai YF, Zhang HM, Zhang Y, Xing DM. A novel H_3PO_4/Nafion-PBI composite membrane for enhanced durability of high temperature PEM fuel cells. J Power Sources 2007;169:259–64.

[157] Zhang W, Gogel V, Friedrich KA, Kerres J. Novel covalently cross-linked poly(etheretherketone) ionomer membranes. J Power Sources 2006;155:3–12.

[158] Kerres J. Covalent-ionically cross-linked poly(etheretherketone)-basic polysulphone blend ionomer membranes. Fuel Cells 2006;6:251–60.

[159] Hasiotis C, Deimede V, Kontoyannis C. New polymer electrolytes based on blends of sulphonated polysulphones with polybenzimidazole. Electrochim Acta 2001;46:2401–6.

[160] Hasiotis C, Li Q, Deimede V, Kallitsis JK, Kontoyannis CG, Bjerrum NJ. Development and characterization of acid-doped polybenzimidazole/sulphonated polysulphone blend polymer electrolytes for fuel cells. J Electrochem Soc 2001;148:A513–9.

[161] Kerres JA, Xing DM, Schonberger F. Comparative investigation of novel FBI blend ionomer membranes from nonfluorinated and partially fluorinated poly arylene ethers. J Polym Sci B: Polym Phys 2006;44:2311–26.

[162] Schönberger F, Chromik A, Kerres J, Hein M, Häring Th, Li Q, et al. Partially fluorinated arylene polyethers and their ternary blends with PBI and H_3PO_4, part I. Synthesis and characterization of polymers and binary blend membranes. Fuel Cells 2008;8:175–87.

[163] Li Q, Jensen JO, Pan C, Bandur V, Nilsson M, Schönberger F, et al. Partially fluorinated arylene polyethers and their ternary blends with PBI and H_3PO_4, part II. Characterizations and fuel cell tests of the ternary membrane. Fuel Cells 2008;8:188–99.

[164] Davis HJ, Thomas NW. Chemical modification of polybenzimidazole semipermeable (Celanese Corporation). US patent 4,020,142 (1977).

[165] Sheratte MB. Linear and cross-linked polybenzimidazoles (Acurex Corporation). US patent 4,154,919 (1979).

[166] Sansone MJ. Crosslinking of polybenzimidazole polymer with divinyl sulfone (Celanese Corporation). US patent 4,666,996 (1987).

[167] Jorgensen BS, Young JS, Espinoza BF. Cross-linked polybenzimidazole membrane for gas separation (The Regents of the University of California). US patent 6,946,015 (2005).

[168] Wang KY, Xiao YC, Chung TS. Chemically modified polybenzimidazole nanofiltration membrane for the separation of electrolytes and cephalexin. Chem Eng Sci 2006;61:5807–17.

[169] Young JS, Long GS, Espinoza BF. Cross-linked polybenzimidazole membrane for gas separation (The Regents of the University of California). US patent 6,997,971 (2006).

[170] Noyé P, Li QF, Pan C, Bjerrum NJ. Cross-linked polybenzimidazole membranes for high temperature proton exchange membrane fuel cells with dichloromethyl phosphoric acid as a cross-linker. Polym Adv Technol 2008;19:1270–5.

[171] Li Q, Pan C, Jensen JO, Noyé P, Bjerrum NJ. Cross-linked polybenzimidazole membranes for fuel cells. Mater Chem 2007;19:350–2.

[172] Staiti P, Minutoli M, Hocevar S. Membranes based on phospho-tungstic acid and polybenzimidazole for fuel cell application. J Power Sources 2000;90:231–5.

[173] Staiti P, Minutoli M. Influence of composition and acid treatment on proton conduction of composite polybenzimidazole membranes. J Power Sources 2001;94:9–13.

[174] Staiti P. Proton conductive membranes based on silicotungstic acid/silica and polybenzimidazole. Mater Lett 2001;47:241–6.

[175] Zaidi SMJ. Preparation and characterization of composite membranes using blends of SPEEK/PBI with boron phosphate. Electrochim Acta 2005;50:4771–7.

[176] Hsu SLC, Chang KC. Synthesis and properties of polybenzoxazole-clay nanocomposites. Polymer 2002;43:4097–101.

[177] Yamazaki Y, Jang MY, Taniyama T. Proton conductivity of zirconium tricarboxybutylphosphonate/PBI nanocomposite membrane. Sci Techn Adv Mater 2004;5:455–9.

[178] Jang MY, Yamazaki Y. Preparation and characterization of composite membranes composed of zirconium tricarboxybutylphosphonate and polybenzimidazole for intermediate temperature operation. J Power Sources 2005;139:2–8.

[179] Heo P, Kajiyama N, Kobayashi K, Nagao M, Sano M, Hibino T. Proton conduction in $Sn_{0.95}Al_{0.05}P_2O_7$–PBI–PTFE composite membrane. Electrochem Solid State Lett 2008;11:B91–5.

[180] Lin HL, Yu TL, Chang WK, Cheng CP, Hu CR, Jung GB. Preparation of a low proton resistance PBI/PTFE composite membrane. J Power Sources 2007;164:481–7.

[181] Kuo PL, Chen WF, Liang WJ. Proton transportation in an organic–inorganic hybrid polymer electrolyte based on a polysiloxane/poly(allylamine) network. J Polym Sci 2005;43A:3359–67.

[182] Hughes CE, Haufe S, Angerstein B, Kalim R, Mahr U, Reiche A, et al. Probing structure and dynamics in poly[2,2'-(m-phenylene)-5,5'-bibenzimidazole] fuel cells with magic-angle spinning NMR. J Phys Chem 2004;108:13626–31.

[183] Musto P, Karasz FE, Macknight WJ. Hydrogen-bonding in poly-benzimidazole polyimide systems—a Fourier-transform infrared investigation using low-molecular-weight monofunctional probes. Polymer 1989;30:1012–21.

[184] Musto P, Karasz FE, Macknight WJ. Fourier-transform infrared-spectroscopy on the thermooxidative degradation of polybenzimidazole and of a polybenzimidazole polyetherimide blend. Polymer 1993;34:2934–45.

[185] Guerra G, Choe S, Williams DJ, Karasz FE, Macknight WJ. Fourier-transform infrared-spectroscopy of some miscible polybenzimidazole polyimide blends. Macromolecules 1998;21:231–4.

[186] Jayakody JRP, Chung SH, Durantino L, Zhang H, Xiao L, Benicewicz BC, et al. NMR studies of mass transport in high-acid-content fuel cell membranes based on phosphoric acid and polybenzimidazole. J Electrochem Soc 2007;154:B242–6.

[187] Voyiatzis GA. Spectroelectrochemical investigation of the ability of PBI-based membranes to be acid doped. In: Presentation at Symposium on high temperature PEM fuel cells. 2005.

[188] Li QF, He RH, Berg RW, Hjuler HA, Bjerrum NJ. Water uptake and acid doping of polybenzimidazoles as electrolyte membranes for fuel cells. Solid State Ionics 2004;168:177–85.

[189] Brooks NW, Duckett RA, Rose J, Ward IM, Clements J. An NMR-study of absorbed water in polybenzimidazole. Polymer 1993;34:4039–42.

[190] He RH, Li QF, Jensen JO, Bjerrum NJ. Doping phosphoric acid in polybenzimidazole membranes for high temperature proton exchange membrane fuel cells. J Polym Sci A: Polym Chem 2007;45:2989–97.

[191] Belohlav LR. Polybenzimidazole. Angew Makromol Chem 1974;40:465–83.

[192] Jaffe M, Haider MI, Menczel J, Rafalko J. Thermal characterization of high-performance PBI and 6F polymers and their alloys. Polym Eng Sci 1992;32:1236–41.

[193] LaConti AB, Hamdan M, McDonald RC. Mechanisms of membrane degradation. In: Vielstichm W, Lamm A, Gasteiger HA, editors. Handbook of fuel cells, vol. 3. John Wiley & Sons Ltd.; 2003. p. 647–62.

[194] Gaudiana RA, Conley RT. Weak-link versus active carbon degradation routes in oxidation of aromatic heterocyclic systems. J Polym Sci 1969;7B:793–8.

[195] He RH, Li QF, Bach A, Jensen JO, Bjerrum NJ. Physicochemical properties of phosphoric acid doped polybenzimidazole membranes for fuel cells. J Membr Sci 2006;277:38–45.

[196] Aharoni SM, Litt MH. Synthesis and some properties of poly-(2,5-trimethylene benzimidazole) and poly-(2,5-trimethylene benzimidazole hydrochloride). J Polym Sci Polymer Chem 1974;12:639–50.

[197] Hoel D, Greenwald E. High protonic conduction of polybenzimidazole films. J Phys Chem 1977;81:2135–6.

[198] Fontanella JJ, Edmondson CA, Wintersgill MC, Wu Y, Greenbaum SG. High-pressure electrical conductivity and NMR studies in variable equivalent weight Nafion membranes. Macromolecules 1996;29:4944–51.

[199] Bouchet R, Miller S, Duclot M, Souquet JL. A thermodynamic approach to proton conductivity in acid-doped polybenzimidazole. Solid State Ionics 2001;145:69–78.

[200] Weng D. Water and methanol transport through polymer electrolytes in elevated temperature fuel cells. PhD thesis. Cleveland, Ohio, USA: Case Western Reserve University; 1996.

[201] Schechter A, Savinell RF. Imidazole and 1-methyl imidazole in phosphoric acid doped polybenzimidazole electrolyte for fuel cells. Solid State Ionics 2002;147:181–7.

[202] Pivovar BS. An overview of electro-osmosis in fuel cell polymer electrolytes. Polymer 2006;47:4194–202.

[203] Zawodzinski TA, Derouin C, Radzinski S, Sherman RJ, Smith VT, Springer TE, et al. Water-uptake by and transport through Nafion 117 membranes. J Electrochem Soc 1993;140:1041–7.

[204] Xie G, Okada T. Water transport behavior in Nafion-117 Membranes. J Electrochem Soc 1995;142:3057–62.

[205] Ise M, Kreuer KD, Maier J. Electroosmotic drag in polymer electrolyte membranes: an electrophoretic NMR study. Solid State Ionics 1999;125:213–23.

[206] Pivovar BS, Smyrl WH, Cussler EL. Electro-osmosis in Nafion 117, polystyrene sulphonic acid, and polybenzimidazole. J Electrochem Soc 2005;152:A53–60.

[207] Weng D, Wainright JS, Landau U, Savinell RF. Electro-osmotic drag coefficient of water and methanol in polymer electrolytes at elevated temperatures. J Electrochem Soc 1996;143:1260–3.

[208] Li QF, Hjuler HA, Bjerrum NJ. Phosphoric acid doped polybenzimidazole membranes: physiochemical characterization and fuel cell applications. J Appl Electrochem 2001;31:773–9.

[209] Pivovar BS, Wang YX, Cussler EL. Pervaporation membranes in direct methanol fuel cells. J Membr Sci 1999;154:155–62.

[210] Wang JT, Wasmus S, Savinell RF. Real-time mass spectrometric study of the methanal crossover in a direct methanol fuel cell. J Electrochem Soc 1996;143:1233–9.

[211] Pu HT, Liu QZ. Methanol permeability and proton conductivity of polybenzimidazole and sulphonated polybenzimidazole. Polym Int 2004;53:1512–6.

[212] Broka K, Ekdunge P. Oxygen and hydrogen permeation properties and water uptake of Nafion 117 membrane and recast film for PEM fuel cell. J Appl Electrochem 1997;27:117–23.

[213] Mecerreyes D, Grande H, Miguel O, Ochoteco E, Marcilla R, Cantero I. Porous polybenzimidazole membranes doped with phosphoric acid: highly proton-conducting solid electrolytes. Chem Mater 2004;16:604–7.

[214] Neyerlin KC, Singh A, Chu D. Kinetic characterization of a Pt-Ni/C catalyst with a phosphoric acid doped PBI membrane in a proton exchange membrane fuel cell. J Power Sources 2008;176:112–7.

[215] Liu ZY, Wainright JS, Litt MH, Savinell RF. Study of the oxygen reduction reaction (ORR) at Pt interfaced with phosphoric acid doped polybenzimidazole at elevated temperature and low relative humidity. Electrochim Acta 2006;51:3914–23.

[216] Zecevic SK, Wainright JS, Litt MH, Gojkovic SL, Savinell RF. Kinetics of O_2 reduction on a Pt electrode covered with a thin film of solid polymer electrolyte. J Electrochem Soc 1997;144:2973–82.

[217] Liu ZY, Wainright JS, Savinell RF. High-temperature polymer electrolytes for PEM fuel cells: study of the oxygen reduction reaction (ORR) at a Pt-polymer electrolyte interface. Chem Eng Sci 2004;59:4833–8.

[218] Zhang J, Tang Y, Song C, Zhang J. Polybenzimidazole-membrane-based PEM fuel cell in the temperature range of 120–200 °C. J Power Sources 2006;172:163–71.

[219] Zelenay P, Scharifker BR, Bockris JO, Gervasio D. A Comparison of the properties of CF_3SO_3H and H_3PO_4 in relation to fuel-cells. J Electrochem Soc 1986;133:2262–7.

[220] Saffarian H, Ross P, Behr F, Gard G. Electrochemical properties of perfluoroalkane disulphonic $[HSO_3(CF_2)NSO_3H]$ acids relevant to fuel-cell technology. J Electrochem Soc 1992;139:2391–7.

[221] Razaq M, Razaq A, Yeager E, DesMarteau DD, Singh S. Perflu-orosulphonimide as an additive in phosphoric-acid fuel-cell. J Electrochem Soc 1989;136:385–90.

[222] Enayetullah MA, OïSullivan EJM, Yeager EB. Oxygen reduction on platinum in mixtures of phosphoric and trifluoromethane sulphonic-acids. J Appl Electrochem 1988;18:763–7.

[223] Li QF. High temperature proton exchange membranes for fuel cells. Dissertation for the degree of Doctor of Technices. Technical University of Denmark; 2006.

[224] Parthasarathy A, Srinivasan S, Appleby AJ, Martin CR. Temperature-dependence of the electrode-kinetics of oxygen reduction at the platinum Nafion interface—a microelectrode investigation. J Electrochem Soc 1992;139:2530–7.

[225] See E-Tek homepage: http://www.etek-inc.com/standard/index. php#GDEHT.

[226] Wang JT, Wainright JS, Savinell RF, Litt M. A direct methanol fuel cell using acid-doped polybenzimidazole as polymer electrolyte. J Appl Electrochem 1996;26:751–6.

[227] Seland F, Berning T, Børresen B, Tunold R. Improving the performance of high-temperature PEM fuel cells based on PBI electrolyte. J Power Sources 2006;160:27–36.

[228] Pan C, Li QF, Jensen JO, He R, Cleemann LN, Nillson M, et al. Preparation and operation of gas diffusion electrodes for high-temperature proton exchange membrane fuel cells. J Power Sources 2007;172:278–86.

[229] Zhai Y, Zhang H, Liu G, Hu J, Yi B. Degradation study on MEA in H_3PO_4/PBI high-temperature PEMFC life test. J Electrochem Soc 2007;154:B72–6.

[230] Hu JW, Zhang HM, Zhai YF, Liu G, Yi BL. 500 h continuous aging life test on PBI/H_3PO_4 high-temperature PEMFC. Int J Hydrogen Energy 2006;31:1855–62.

[231] Zhai YF, Zhang HM, Xing DM, Shao ZG. The stability of Pt/C catalyst in H_3PO_4/PBI PEMFC during high temperature life test. J Power Sources 2007;164:126–33.

[232] Kim HJ, An SJ, Kim JY, Moon JK, Cho SY, Eun YC, et al. Polybenzimidazoles for high temperature fuel cell applications. Macromol Rapid Commun 2004;25:1410–3.

[233] Savinell R, Yeager E, Tryk D, Landau U, Wainright J, Weng D, et al. A polymer electrolyte for operation at temperatures up to 200 °C. J Electrochem Soc 1994;141:L46–8.

[234] Li QF, Hjuler HA, Bjerrum NJ. Oxygen reduction on carbon supported platinum catalysts in high temperature polymer electrolytes. Electrochim Acta 2000;45:4219–26.

[235] Park JO, Hong SG, Kim TY, Kwon KJ, Suh SH, Cho MD, et al. Role of binders in high temperature PEMFC electrodes. ECS Trans 2006;3(1):447–51.

[236] Lobato J, Rodrigo MA, Linares JJ, Scott K. Effect of the catalytic ink preparation method on the performance of high temperature polymer electrolyte membrane fuel cells. J Power Sources 2006;157:284–92.

[237] Jalani NH, Ramani M, Ohlsson K, Buelte S, Pacifico G, Pollard R, et al. Performance analysis and impedance spectral signatures of high temperature PBI-phosphoric acid gel membrane fuel cells. J Power Sources 2006;160:1096–103.

[238] Staudt R. Development of polybenzimidazole-based high temperature membrane and electrode assemblies for stationary applications. 2006 Annual progress report [http://www.hydrogen.energy. gov/pdfs/progress06/v_b_5_staudt.pdf].

[239] Reiche A. Sartorius HT-PEMFC membrane electrode assembly (abstracts 502 and 507). In: The 2006 fuel cell seminar. 2006.

[240] Stolten D, Wannek C, Dohle H, Blum L, Mergel J, Peters R. Strategy, status and outlook for HTPEFC development for APU application (abstract 162). In: Fuel cell seminar 2007. 2007.

[241] Wang JT, Wasmus S, Savinell RF. Evaluation of ethanol, 1-propanol, and 5-propanol in a direct oxidation polymer-electrolyte fuel cell - A real-time mass spectrometry study. J Electrochem Soc 1995;142:4218–24.

[242] Wang JT, Lin WF, Weber M, Wasmus S, Savinell RF. Trimethoxymethane as an alternative fuel for a direct oxidation PBI polymer electrolyte fuel cell. Electrochim Acta 1998;43:3821–8.

[243] Weber M, Wang JT, Wasmus S, Savinell RF. Formic acid oxidation in a polymer electrolyte fuel cell—a real-time mass-spectrometry study. J Electrochem Soc 1996;143:L158–60.

[244] Wang CP, Chua HS, Yan YY, Hsueh KL. Transient evolution of carbon monoxide poisoning effect of PBI membrane fuel cells. J Power Sources 2007;170:235–41.

[245] Lee SJ, Mukerjee S, Ticianelli EA, McBreen J. Electrocatalysis of CO tolerance in hydrogen oxidation reaction in PEM fuel cells. Electrochim Acta 1999;44:3283–93.

[246] Gottesfeld S, Pafford J. A new approach to the problem of carbon-monoxide poisoning in fuel-cells operating at low-temperatures. J Electrochem Soc 1988;135:2651–2.

[247] Oetjen HF, Schmidt VM, Stimming U, Trila F. Performance data of a proton exchange membrane fuel cell using H_2/CO as fuel gas. J Electrochem Soc 1996;143:3838–42.

[248] Schmidt TJ, Baurmeister J. Durability and reliability in high-temperature reformed hydrogen PEFCs. ECS Trans 2006; 3(1):861–9.

[249] Mohtadi R, Lee WK, Cowan S, Van Zee JW, Murthy M. Effects of hydrogen sulphide on the performance of a PEMFC. Electrochem Solid State Lett 2003;6:A272–4.

[250] Mohtadi R, Lee WK, Van Zee JW. The effect of temperature on the adsorption rate of hydrogen sulphide on Pt anodes in a PEMFC. Appl Catal 2005;56B:37–42.

[251] Shi WY, Yi BL, Hou M, Jing FN, Yu HM, Ming PW. The influence of hydrogen sulphide on proton exchange membrane fuel cell anodes. J Power Sources 2007;164:272–7.

[252] Shi WY, Yi BL, Hou M, Jing FN, Ming PW. Hydrogen sulphide poisoning and recovery of PEMFC Pt-anodes. J Power Sources 2007;165:814–8.

[253] Hubner G, Huslage J, Seyfried F. Volkswagen contribution to PBI membranes and fuel cells. Results kindly provided by the Volkswagen fuel cell research group; 2008.

[254] Li QF, Hjuler HA, Hasiotis C, Kallitsis JK, Kontoyannis CG, Bjerrum NJ. A quasi-direct methanol fuel cell system based on blend polymer membrane electrolytes. Electrochem Solid State Lett 2002;5:A125–8.

[255] Morse JD, Upadhye RS, Graff RT, Spadaccini C, Park HG, Hart EK. A MEMS-based reformed methanol fuel cell for portable power. J Micromech Microeng 2007;17:S237–42.

[256] Jensen CM, Gross KJ. Development of catalytically enhanced sodium aluminum hydride as a hydrogen-storage material. Appl Phys 2001;A72:213–9.

[257] Chan JP, Dedrick DE, Gross KJ, Ng GL. Compact fuel cell system utilizing a combination of hydrogen storage materials for optimized performance. Technical report SAND2004-6347. Sandia National Laboratory; 2004.

[258] Borup R, Meyers J, Pivovar B, Kim YS, Mukundan R, Garland N, et al. Scientific aspects of polymer electrolyte fuel cell durability and degradation. Chem Rev 2007;107:3904–51.

[259] Schmidt TJ, Baurmeister J. Properties of high-temperature PEFC Celtec_P1000 MEAs in start/stop operation mode. J Power Sources 2008;176:428–34.

[260] Wannek C, Kohnen B, Oetjen HF, Lippert H, Mergel J. Durability of ABPBI-based MEAs for high temperature PEMFCs at different operating conditions. Fuel Cells 2008;8:87–95.

[261] Calundann G. Market introduction of reformed hydrogen fuel cells (RHFC) based on high temperature Celtec_P1000 MEAs (abstract 409). In: The 2006 fuel cell seminar. 2006.

[262] Yasuda K, Taniguchi A, Akita T, Ioroi T, Siroma Z. Platinum dissolution and deposition in the polymer electrolyte membrane of a PEM fuel cell as studied by potential cycling. Phys Chem Chem Phys 2006;8:746–52.

[263] Xie J, Wood DL, Wayne DM, Zawodzinski TA, Atanassov P, Borup RL. Durability of PEFCs at high humidity conditions. J Electrochem Soc 2005;152:A104–13.

[264] Qi ZG, Buelte S. Effect of open circuit voltage on performance and degradation of high temperature PBI-H_3PO_4 fuel cells. J Power Sources 2006;161:1126–32.

[265] Mathias MF, Makharia R, Gasteiger HA, Conley JJ, Fuller TJ, Gittleman CJ, et al. Two fuel cell cars in every garage? Electrochem Soc Interface 2005;14(3):24–35.

[266] Landsman DA, Luczak FJ. Catalyst studies and coating technologies. In: Vielstichm W, Lamm A, Gasteiger HA, editors. Handbook of fuel cells, vol. 4. John Wiley & Sons Ltd.; 2003. p. 811–31.

[267] Cleemann LN, Li QF, Jensen JO, Pan C, Liu CD, Dai S, et al. Catalyst degradation in high temperature proton exchange membrane fuel cells based on acid doped polybenzimidazole membranes. J Electrochem Soc; submitted for publication.

[268] Liu G, Zhang HM, Zhai YF, Zhang Y, Xu DY, Shao ZG. Pt_4ZrO_2/C cathode catalyst for improved durability in high temperature PEMFC based on H_3PO_4 doped PBI. Electrochem Commun 2007;9:135–41.

[269] Liu G, Zhang HM, Zhong HX, Hu JW, Xu DY, Shao ZG. A novel sintering resistant and corrosion resistant Pt_4ZrO_2/C catalyst for high temperature PEMFCs. Electrochim Acta 2006;51: 5710–4.